CLIMATE DIAGNOSTICS BULLETIN

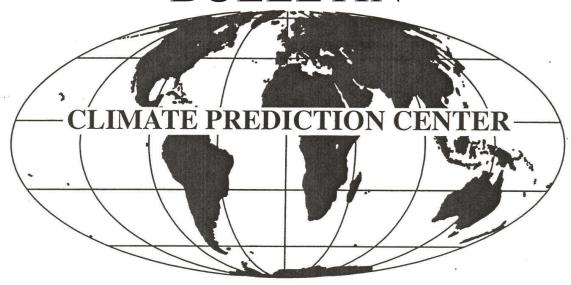**CLIMATE PREDICTION CENTER**

APRIL 2021

NEAR REAL-TIME OCEAN / ATMOSPHERE

Monitoring, Assessments, and Prediction

U.S. DEPARTMENT OF COMMERCE
National Oceanic and Atmospheric Administration
National Weather Service

National Centers for Environmental Prediction

CLIMATE DIAGNOSTICS BULLETIN

CLIMATE PREDICTION CENTER
Attn: Climate Diagnostics Bulletin
Room 3116, NCWCP
5830 University Research Court
College Park, MD 20740

Software: Most of the bulletin figures generated at CPC are created using the Grid Analysis and Display System (GrADS).

- Climate Diagnostics Bulletin available on the World Wide Web

The CDB is available on the World Wide Web. The address of the online version of the CDB is:

http://www.cpc.ncep.noaa.gov/products/CDB

If you have any problems accessing the bulletin, contact Dr. Wei Shi by E-mail:

Wei.Shi@noaa.gov

Table of Contents

TROPICS

FIGURE

Time Series
Southern Oscillation Index (SOI)	T1
Tahiti and Darwin SLP Anomalies	T1
OLR Anomalies	T1
CDAS/Reanalysis SOI & Equatorial SOI	T2
200-hPa Zonal Wind Anomalies	T3
500-hPa Temperature Anomalies	T3
30-hPa and 50-hPa Zonal Wind Anomalies	T3
850-hPa Zonal Wind Anomalies	T4
Equatorial Pacific SST Anomalies	T5

Time-Longitude Sections
Mean and Anomalous Sea Level Pressure	T6
Mean and Anomalous 850-hPa Zonal Wind	T7
Mean and Anomalous OLR	T8
Mean and Anomalous SST	T9
Pentad SLP Anomalies	T10
Pentad OLR Anomalies	T11
Pentad 200-hPa Velocity Potential Anomalies	T12
Pentad 850-hPa Zonal Wind Anomalies	T13
Anomalous Equatorial Zonal Wind	T14
Mean and Anomalous Depth of the 20°C Isotherm	T15

Mean & Anomaly Fields
Depth of the 20°C Isotherm	T16
Subsurface Equatorial Pacific Temperatures	T17
SST	T18
SLP	T19
850-hPa Vector Wind	T20
200-hPa Vector Wind	T21
200-hPa Streamfunction	T22
200-hPa Divergence	T23
200-hPa Velocity Potential and Divergent Wind	T24
OLR	T25
SSM/I Tropical Precipitation Estimates	T26
Cloud Liquid Water	T27
Precipitable Water	T28
Divergence & E-W Divergent Circulation	T29 - T30
Pacific Zonal Wind & N-S Divergent Circulation	T31 - T32

Appendix 1: Outside Contributions
Tropical Drifting Buoys	A1.1

4

Tropical Highlights - April 2021

During April 2021, sea surface temperatures (SSTs) were near-average in the central equatorial Pacific and below-average across the eastern equatorial Pacific (Fig. T18). The latest monthly Niño indices were -0.8°C for the Niño 1+2 region, -0.5°C for the Niño 3.4 region and -0.2°C for the Niño 4 region (Fig. T5, Table T2). The depth of the oceanic thermocline (measured by the depth of the 20°C isotherm) was above-average across much of the equatorial Pacific (Figs. T15, T16). The corresponding sub-surface temperatures were 1-3°C above-average (Fig. T17).

Also during April, the lower-level easterly winds and the upper-level westerly winds were above-average across the east-central and eastern equatorial Pacific (Fig. T20, Fig. T21). Meanwhile, tropical convection was near-average over the central equatorial Pacific and suppressed over Indonesia (Figs. T25, E3). Collectively, these oceanic and atmospheric anomalies reflected a transition towards ENSO-neutral conditions.

For the latest status of the ENSO cycle see the ENSO Diagnostic Discussion at:
http://www.cpc.ncep.noaa.gov/products/analysis_monitoring/enso_advisory/index.html

Month	SLP Anomalies		Tahiti minus Darwin SOI	850-hPa Zonal Wind Index			200-hPa Wind Index	OLR Index
	Tahiti	Darwin		5N-5S 135E-180	5N-5S 175W-140W	5N-5S 135W-120W	5N-5S 165W-110W	5N-5S 160E-160W
APR 21	0.5	-0.2	0.3	-0.1	1.2	1.4	1.9	0.0
MAR 21	0.4	-0.2	0.4	1.3	0.8	0.7	1.3	1.4
FEB 21	0.9	-1.8	1.5	0.4	1.3	1.4	2.3	1.1
JAN 21	2.5	-1.1	1.9	2.1	1.6	-0.6	3.3	2.4
DEC 20	2.5	-0.9	1.8	1.8	1.8	0.0	2.3	2.0
NOV 20	1.4	0.1	0.7	1.7	1.4	0.3	0.4	1.5
OCT 20	0.1	-0.8	0.5	1.0	1.7	2.0	1.6	1.2
SEP 20	1.1	-0.6	0.9	1.1	1.4	1.4	1.5	0.9
AUG 20	1.1	-0.9	1.1	0.5	0.4	0.5	0.0	0.9
JUL 20	0.1	-0.7	0.4	1.1	1.0	1.1	0.7	0.9
JUN 20	-0.8	0.0	-0.4	0.5	0.2	1.1	0.0	1.1
MAY 20	1.7	0.9	0.4	0.8	1.2	1.7	1.0	0.7
APR 20	1.0	0.6	0.2	0.4	1.1	0.9	0.9	0.7

TABLE T1 - Atmospheric index values for the most recent 12 months. Indices are standardized by the mean annual standard deviation, except for the Tahiti and Darwin SLP anomalies which are in units of hPa. Positive (negative) values of 200-hPa zonal wind index imply westerly (easterly) anomalies. Positive (negative) values of 850-hPa zonal wind indices imply easterly (westerly) anomalies. Anomalies are departures from the 1981-2010 base period means.

Month	PACIFIC SST								ATLANTIC SST				GLOBAL	
	Niño 1+2 0-10S 90W-80W		Niño 3 5N-5S 150W-90W		Niño 3.4 5N-5S 170W-120W		Niño 4 5N-5S 160E-150W		N.ATL 5N-20N 60W-30W		S. ATL 0-20S 30W-10E		TROPICS 10N-10S 0-360	
APR 21	-0.8	24.9	-0.7	27.0	-0.5	27.4	-0.2	28.5	-0.2	25.8	-0.1	27.0	-0.1	28.6
MAR 21	-0.3	26.5	-0.4	26.8	-0.5	26.8	-0.6	27.8	0.1	25.7	-0.4	26.8	-0.2	28.2
FEB 21	-0.7	25.5	-0.6	25.8	-0.9	25.8	-1.0	27.2	0.3	26.0	-0.5	26.1	-0.3	27.7
JAN 21	-0.8	23.7	-0.7	25.0	-1.1	25.5	-1.2	27.1	0.7	26.7	-0.1	25.5	-0.3	27.4
DEC 20	-0.7	22.2	-0.8	24.4	-1.0	25.5	-0.8	27.7	0.5	27.3	-0.4	24.3	-0.1	27.6
NOV 20	-0.7	20.9	-1.2	23.8	-1.3	25.3	-0.7	27.9	0.3	27.9	-0.2	23.7	-0.1	27.6
OCT 20	-1.2	19.6	-1.3	23.6	-1.4	25.3	-0.8	27.9	0.3	28.4	-0.1	23.2	-0.1	27.4
SEP 20	-0.9	19.5	-1.3	23.6	-1.0	25.8	-0.4	28.3	0.3	28.4	-0.1	22.9	-0.0	27.2
AUG 20	-0.9	19.7	-0.5	24.5	-0.6	26.2	-0.2	28.5	0.4	28.2	0.3	23.4	0.2	27.4
JUL 20	-1.2	20.5	-0.5	25.1	-0.3	26.9	0.1	28.9	0.5	27.8	0.0	23.8	0.2	27.7
JUN 20	-0.7	22.1	-0.7	25.8	-0.4	27.3	0.2	29.1	0.6	27.3	0.4	25.3	0.3	28.3
MAY 20	0.1	24.4	-0.2	26.9	-0.2	27.6	0.2	29.0	0.2	26.6	0.7	26.9	0.4	28.9
APR 20	0.4	26.0	0.5	28.0	0.5	28.3	0.8	29.3	0.4	26.4	0.2	27.2	0.5	29.1

TABLE T2. Mean and anomalous sea surface temperature (°C) for the most recent 12 months. Anomalies are departures from the 1981–2010 adjusted OI climatology (Smith and Reynolds 1998, *J. Climate*, **11**, 3320-3323).
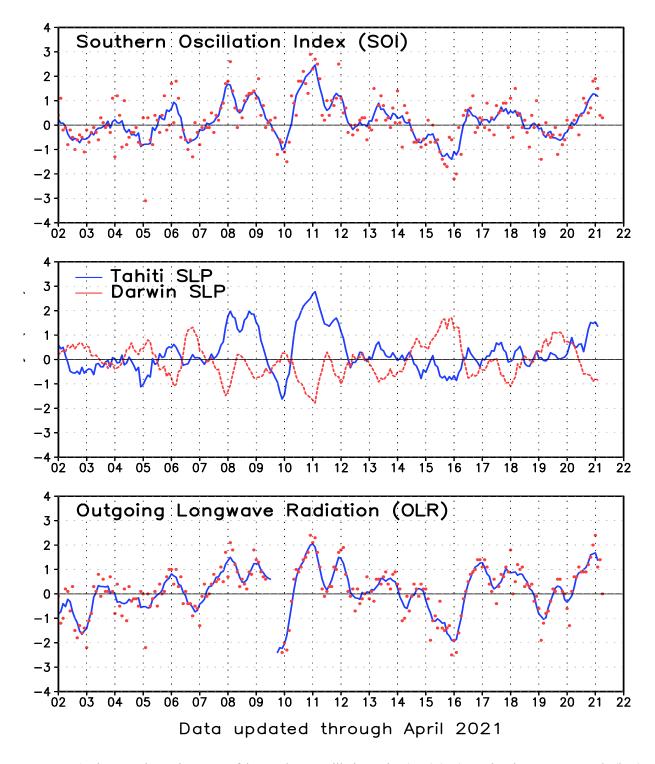
8

FIGURE T1. Five-month running mean of the Southern Oscillation Index (SOI) (top), sea-level pressure anomaly (hPa) at Darwin and Tahiti (middle), and outgoing longwave radiation anomaly (OLR) averaged over the area 5N-5S, 160E-160W (bottom). Anomalies in the top and middle panels are departures from the 1981-2010 base period means and are normalized by the mean annual standard deviation. Anomalies in the bottom panel are departures from the 1981-2010 base period means. Individual monthly values are indicated by "x"s in the top and bottom panels. The x-axis labels are centered on July.

FIGURE T2. Three-month running mean of a CDAS/Reanalysis-derived (a) Southern Oscillation Index (RSOI), (b) standardized pressure anomalies near Tahiti (solid) and Darwin (dashed), (c) an equatorial SOI ([EPAC] - [INDO]), and (d) standardized equatorial pressure anomalies for (EPAC) (solid) and (INDO) (dashed). Anomalies are departures from the 1981-2010 base period means and are normalized by the mean annual standard deviation. The equatorial SOI is calculated as the normalized difference between the standardized anomalies averaged between 5°N–5°S, 80°W–130°W (EPAC) and 5°N–5°S, 90°E–140°E (INDO).
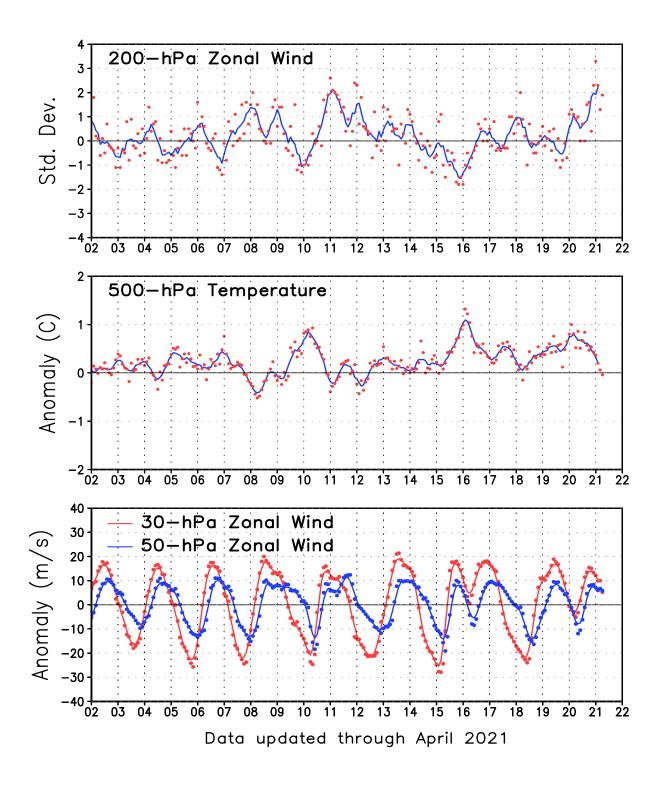
10

FIGURE T3. Five-month running mean (solid lines) and individual monthly mean (dots) of the 200-hPa zonal wind anomalies averaged over the area 5N-5S, 165W-110W (top), the 500-hPa virtual temperature anomalies averaged over the latitude band 20N-20S (middle), and the equatorial zonally-averaged zonal wind anomalies at 30-hPa (red) and 50-hPa (blue) (bottom). In the top panel, anomalies are normalized by the mean annual standard deviation. Anomalies are departures from the 1981-2010 base period means. The x-axis labels are centered on January.
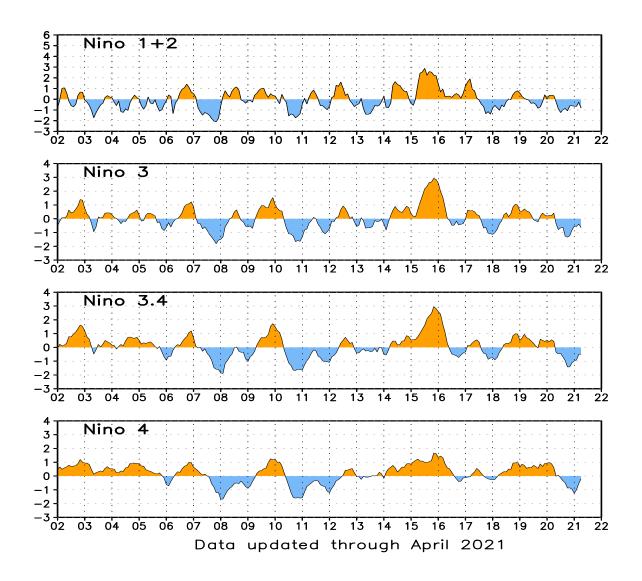
FIGURE T4. Five-month running mean (solid line) and individual monthly mean (dots) of the standardized 850-hPa zonal wind anomaly index in the latitude belt 5N-5S for 135E-180 (top), 175W-140W (middle) and 135W-120W (bottom). Anomalies are departures from the 1981-2010 base period means and are normalized by the mean annual standard deviation. The x-axis labels are centered on January. Positive (negative) values indicate easterly (westerly) anomalies.
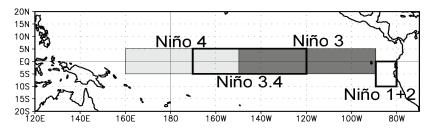
FIGURE T5. Nino region indices, calculated as the area-averaged sea surface temperature anomalies (C) for the specified region. The Nino 1+2 region (top) covers the extreme eastern equatorial Pacific between 0-10S, 90W-80W. The Nino-3 region (2nd from top) spans the eastern equatorial Pacific between 5N-5S, 150W-90W. The Nino 3.4 region 3rd from top) spans the east-central equatorial Pacific between 5N-5S, 170W-120W. The Nino 4 region (bottom) spans the date line and covers the area 5N-5S, 160E-150W. Anomalies are departures from the 1981-2010 base period monthly means *(Smith and Reynolds 1998, J. Climate, 11, 3320-3323)*. Monthly values of each index are also displayed in Table 2.
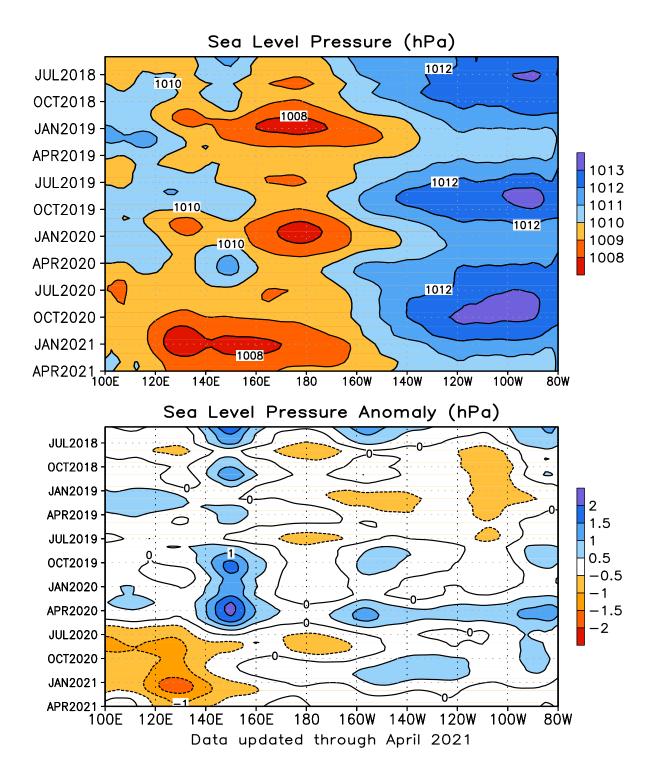
13

FIGURE T6. Time-longitude section of mean (top) and anomalous (bottom) sea level pressure (SLP) averaged between 5N-5S (CDAS/Reanalysis). Contour interval is 1.0 hPa (top) and 0.5 hPa (bottom). Dashed contours in bottom panel indicate negative anomalies. Anomalies are departures from the 1981-2010 base period monthly means. The data are smoothed temporally using a 3-month running average.
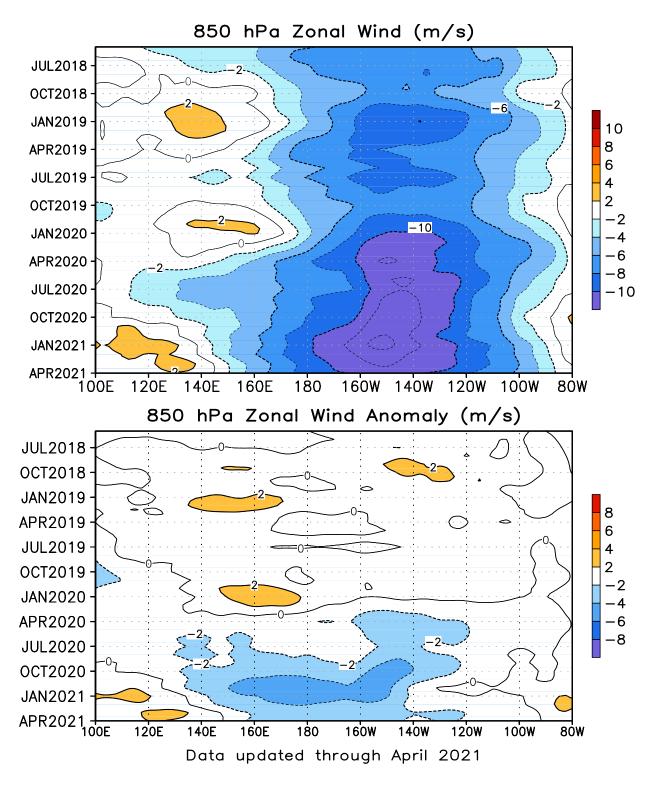
850 hPa Zonal Wind (m/s)

850 hPa Zonal Wind Anomaly (m/s)

Data updated through April 2021

FIGURE T7. Time-longitude section of mean (top) and anomalous (bottom) 850-hPa zonal wind averaged between 5N-5S (CDAS/Reanalysis). Contour interval is 2 ms⁻¹. Blue shading and dashed contours indicate easterlies (top) and easterly anomalies (bottom). Anomalies are departures from the 1981-2010 base period monthly means. The data are smoothed temporally using a 3-month running average.

Outgoing Longwave Radiation (W/m2)

Outgoing Longwave Radiation Anomaly (W/m2)
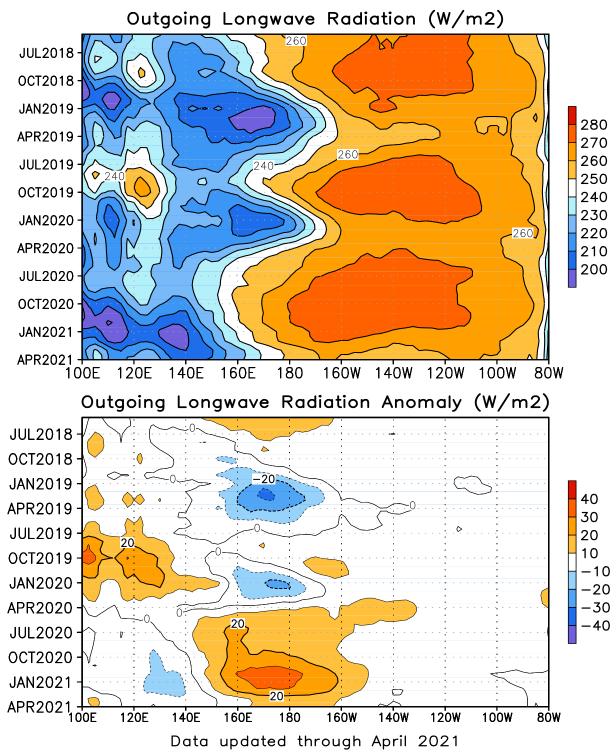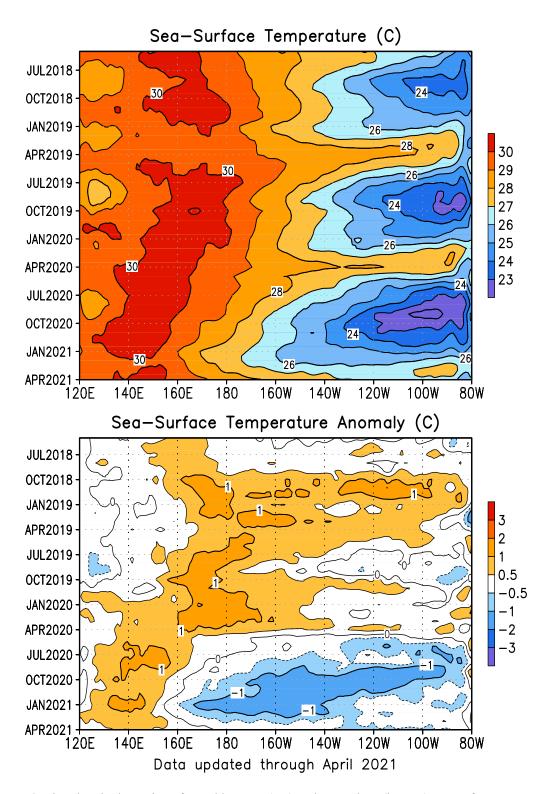
Data updated through April 2021

FIGURE T8. Time-longitude section of mean (top) and anomalous (bottom) outgoing longwave radiation (OLR) averaged between 5N-5S. Contour interval is 10 Wm^{-2}. Dashed contours in bottom panel indicate negative OLR anomalies. Anomalies are departures from the 1981-2010 base period monthly means. The data are smoothed temporally using a 3-month running average.

Sea−Surface Temperature (C)

Sea−Surface Temperature Anomaly (C)

Data updated through April 2021

FIGURE T9. Time-longitude section of monthly mean (top) and anomalous (bottom) sea surface temperature (SST) averaged between 5N-5S. Contour interval is 1C (top) and 0.5C (bottom). Dashed contours in bottom panel indicate negative anomalies. Anomalies are departures from the 1981-2010 base period means (Smith and Reynolds 1998, *J. Climate*, **11**, 3320-3323).
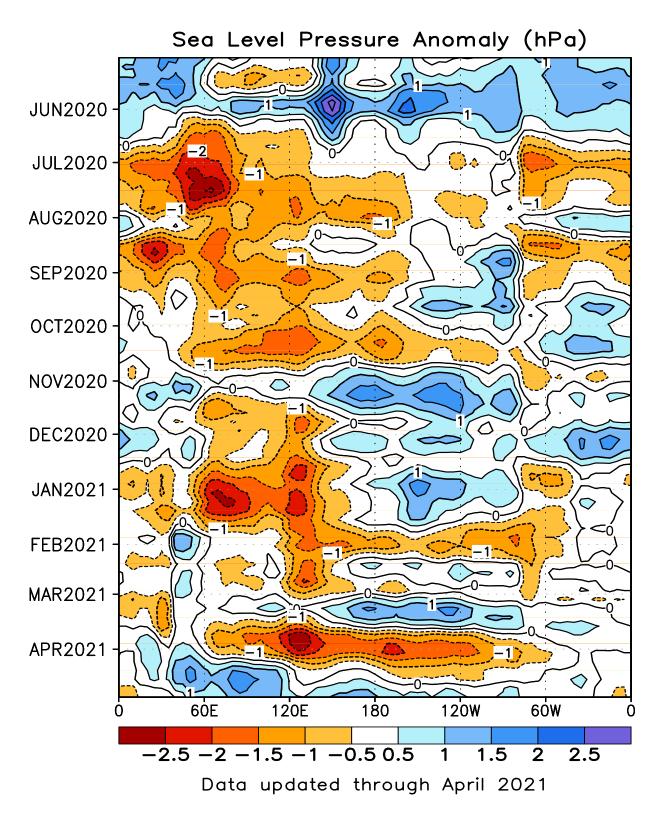
17

FIGURE T10. Time-longitude section of anomalous sea level pressure (hPa) averaged between 5N-5S (CDAS/Re-anaysis). Contour interval is 1 hPa. Dashed contours indicate negative anomalies. Anomalies are departures from the 1981-2010 base period pentad means. The data are smoothed temporally using a 3-point running average.
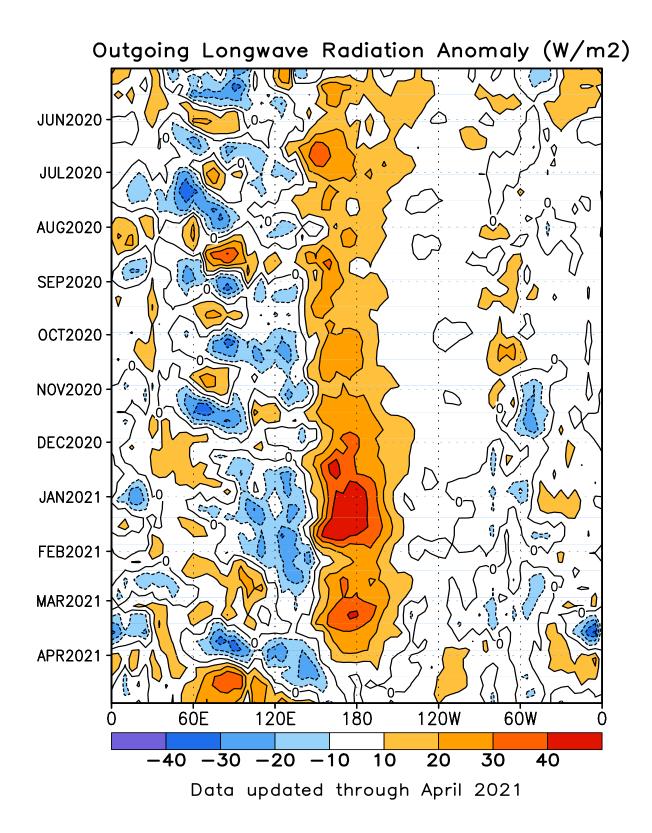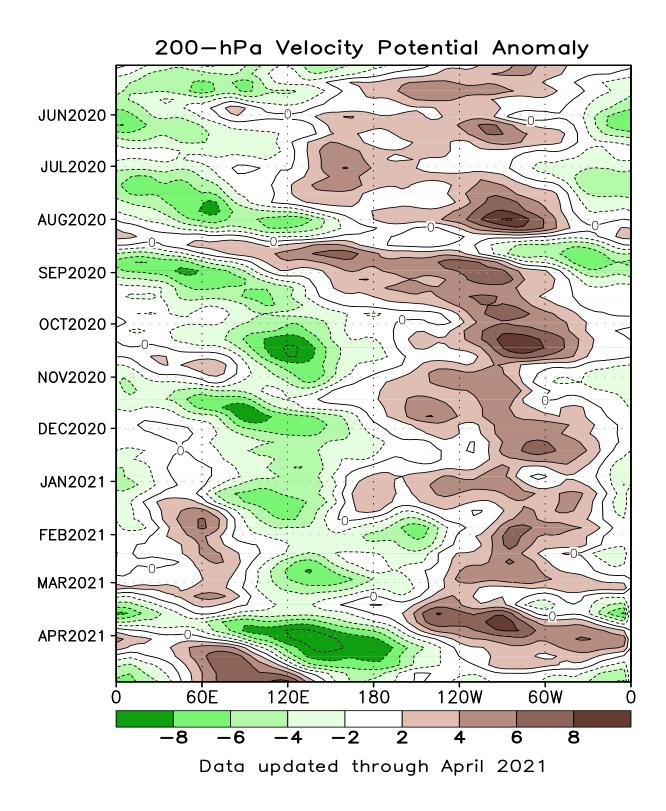
Outgoing Longwave Radiation Anomaly (W/m2)

Data updated through April 2021

FIGURE T11. Time-longitude section of anomalous outgoing longwave radiation averaged between 5N-5S. Contour interval is 15 Wm^{-2}. Dashed contours indicate negative anomalies. Anomalies are departures from the 1981-2010 base period pentad means. The data are smoothed temporally using a 3-point running average.
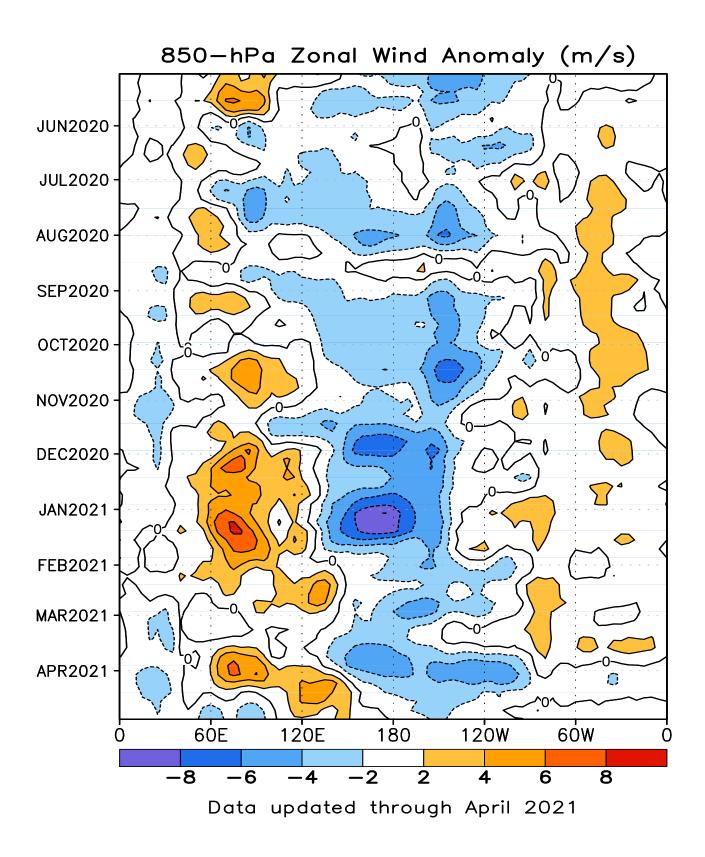
200-hPa Velocity Potential Anomaly

Data updated through April 2021

FIGURE T12. Time-longitude section of anomalous 200-hPa velocity potential averaged between 5N-5S (CDAS/Re-analysis). Contour interval is 3 x 10^6 m^{2}s^{-1}. Dashed contours indicate negative anomalies. Anomalies are departures from the 1981-2010 base period pentad means. The data are smoothed temporally using a 3-point running average.
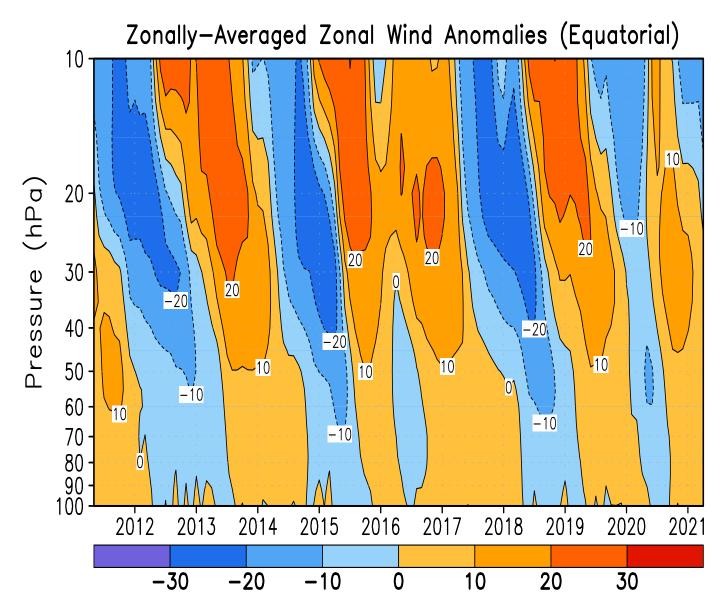
FIGURE T13. Time-longitude section of anomalous 850-hPa zonal wind averaged between 5N-5S (CDAS/Reanalysis). Contour interval is 2 ms^{-1}. Dashed contours indicate negative anomalies. Anomalies are departures from the 1981-2010 base period pentad means. The data are smoothed temporally by using a 3-point running average.

Zonally-Averaged Zonal Wind Anomalies (Equatorial)

FIGURE T14. Equatorial time-height section of anomalous zonally-averaged zonal wind (m s⁻¹) (CDAS/Reanalysis). Contour interval is 10 ms⁻¹. Anomalies are departures from the 1981-2010 base period monthly means.
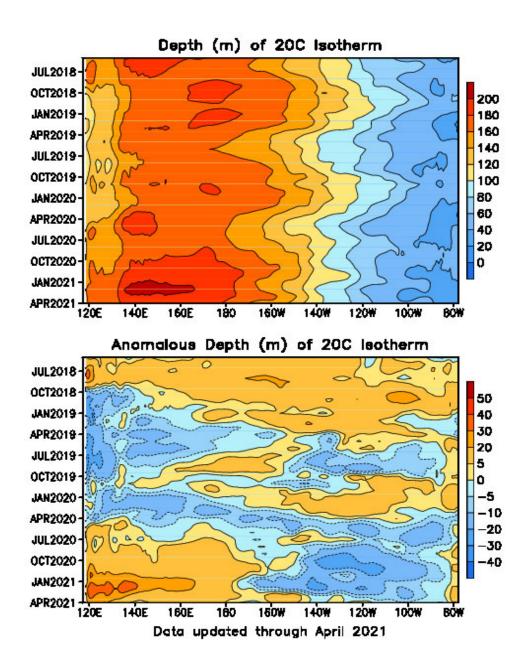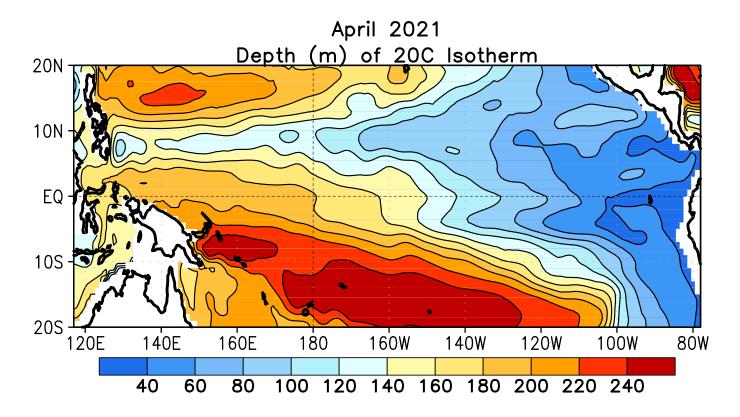
Depth (m) of 20C Isotherm

Anomalous Depth (m) of 20C Isotherm

Data updated through April 2021

FIGURE T15. Mean (top) and anomalous (bottom) depth of the 20C isotherm averaged between 5N-5S in the Pacific Ocean. Data are derived from the NCEP's global ocean data assimilation system which assimilates oceanic observations into an oceanic GCM (Behringer, D. W., and Y. Xue, 2004: Evaluation of the global ocean data assimilation system at NCEP: The Pacific Ocean. AMS 84th Annual Meeting, Seattle, Washington, 11-15). The contour interval is 10 m. Dashed contours in bottom panel indicate negative anomalies. Anomalies are departures from the 1981-2010 base period means.

April 2021
Depth (m) of 20C Isotherm

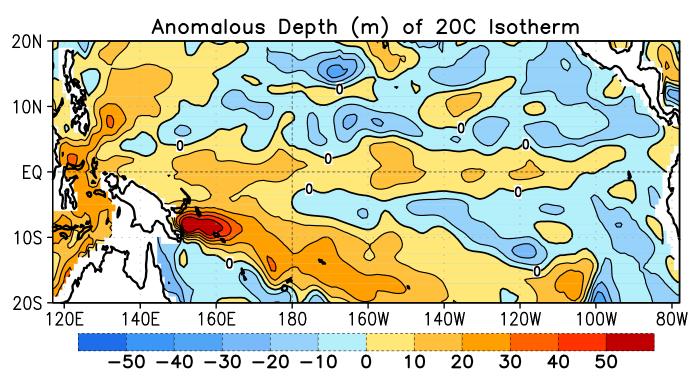## Anomalous Depth (m) of 20C Isotherm

FIGURE T16. Mean (top) and anomalous (bottom) depth of the 20°C isotherm for APR 2021. Contour interval is 40 m (top) and 10 m (bottom). Dashed contours in bottom panel indicate negative anomalies. Data are derived from the NCEP's global ocean data assimilation system version 2 which assimilates oceanic observations into an oceanic GCM (Xue, Y. and Behringer, D.W., 2006: Operational global ocean data assimilation system at NCEP, to be submitted to BAMS). Anomalies are departures from the 1981–2010 base period means.
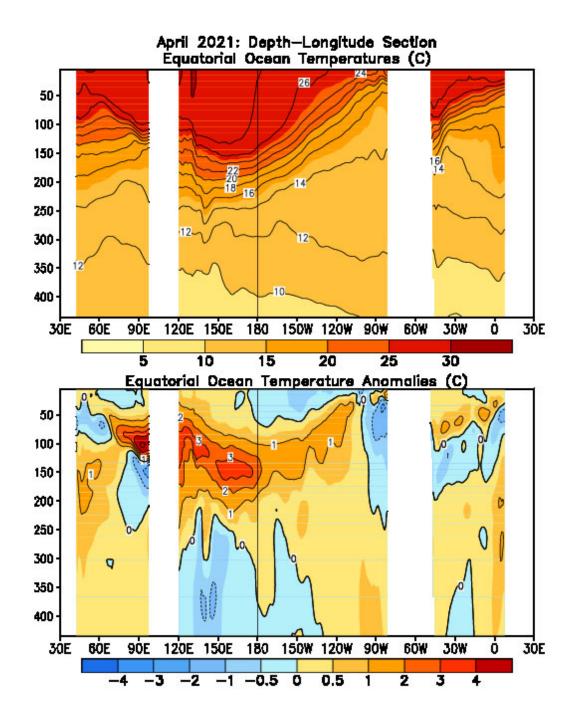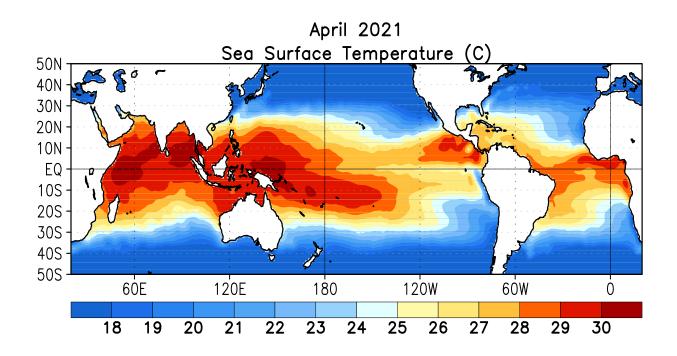
FIGURE T17. Equatorial depth-longitude section of ocean temperature (top) and ocean temperature anomalies (bottom) for APR 2021. Contour interval is 1°C. Dashed contours in bottom panel indicate negative anomalies. Data are derived from the NCEP's global ocean data assimilation system version 2 which assimilates oceanic observations into an oceanic GCM (Xue, Y. and Behringer, D.W., 2006: Operational global ocean data assimilation system at NCEP, to be submitted to BAMS). Anomalies are departures from the 1981–2010 base period means.
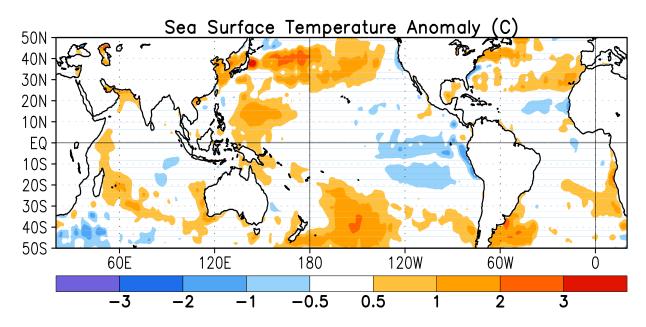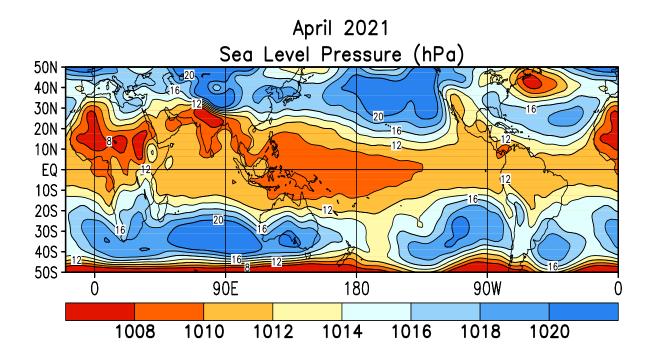
FIGURE T18. Mean (top) and anomalous (bottom) sea surface temperature (SST). Anomalies are departures from the 1981-2010 base period monthly means (Smith and Reynolds 1998, *J. Climate*, **11**, 3320-3323).

April 2021
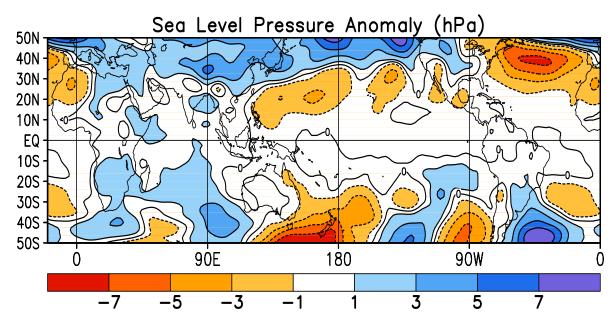## Sea Level Pressure (hPa)

Sea Level Pressure Anomaly (hPa)

FIGURE T19. Mean (top) and anomalous (bottom) sea level pressure (SLP) (CDAS/Reanalysis). In top panel, 1000 hPa has been subtracted from contour labels, contour interval is 2 hPa, and values below 1000 hPa are indicated by dashed contours. In bottom panel, anomaly contour interval is 1 hPa and negative anomalies are indicated by dashed contours. Anomalies are departures from the 1981-2010 base period monthly means.
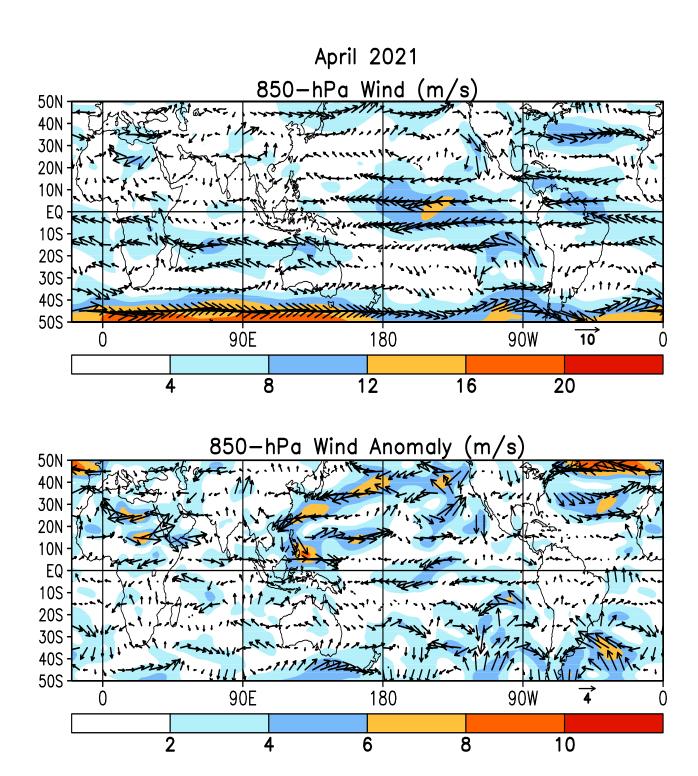
April 2021
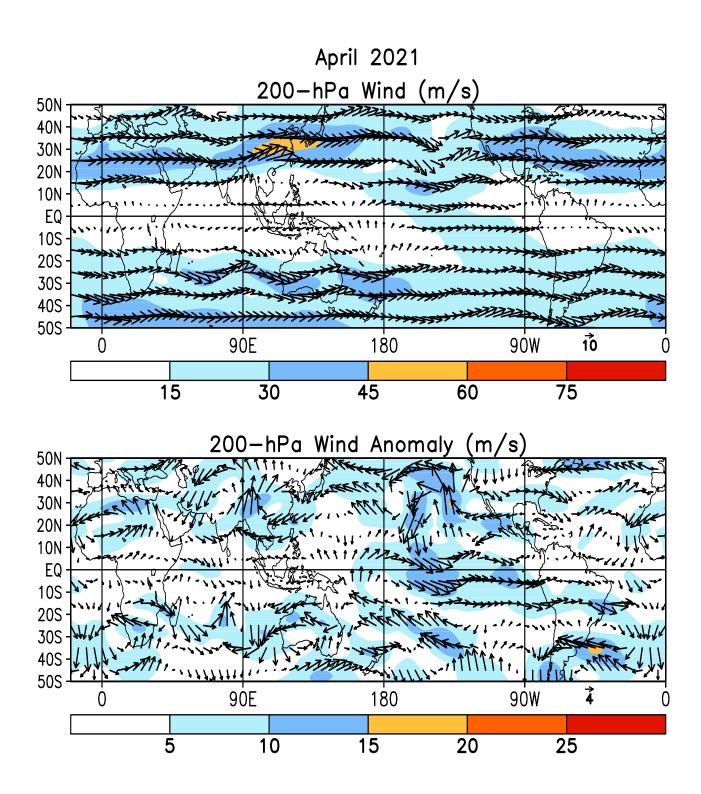## 850-hPa Wind (m/s)

850-hPa Wind Anomaly (m/s)

FIGURE T20. Mean (top) and anomalous (bottom) 850-hPa vector wind (CDAS/Reanaysis) for APR 2021. Contour interval for isotachs is 4 ms^{-1} (top) and 2 ms^{-1} (bottom). Anomalies are departures from the 1981-2010 base period monthly means.

April 2021
200-hPa Wind (m/s)

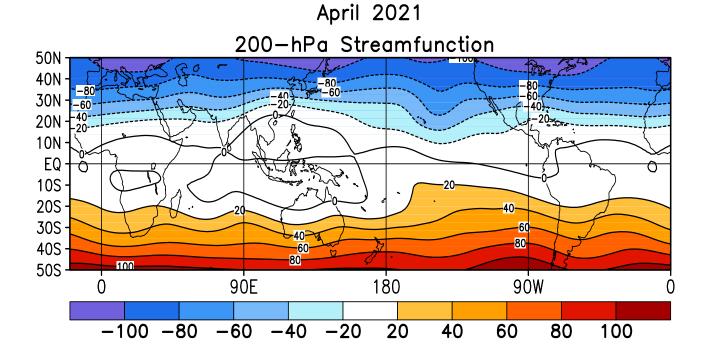
200-hPa Wind Anomaly (m/s)

FIGURE T21. Mean (top) and anomalous (bottom) 200-hPa vector wind (CDAS/Reanalysis) for APR 2021. Contour interval for isotachs is 15 ms^{-1} (top) and 5 ms^{-1} (bottom). Anomalies are departures from 1981-2010 base period monthly means.
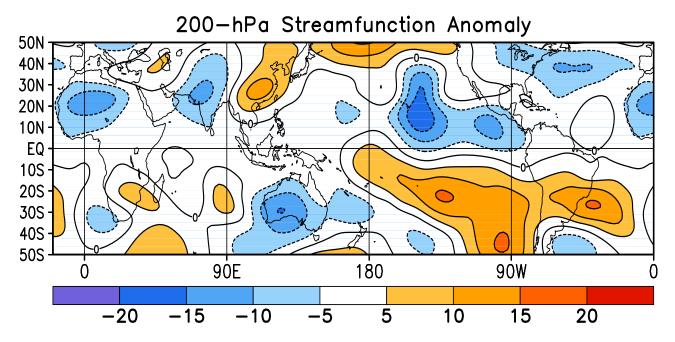
April 2021

200-hPa Streamfunction

200-hPa Streamfunction Anomaly

FIGURE T22. Mean (top) and anomalous (bottom) 200-hPa streamfunction (CDAS/Reanalysis). Contour interval is 20×10^6 m²s⁻¹ (top) and 5×10^6 m²s⁻¹ (bottom). Negative (positive) values are indicated by dashed (solid) lines. The non-divergent component of the flow is directed along the contours with speed proportional to the gradient. Thus, high (low) stream function corresponds to high (low) geopotential height in the Northern Hemisphere and to low (high) geopotential height in the Southern Hemisphere. Anomalies are departures from the 1981-2010 base period monthly means.

April 2021

200-hPa Divergence
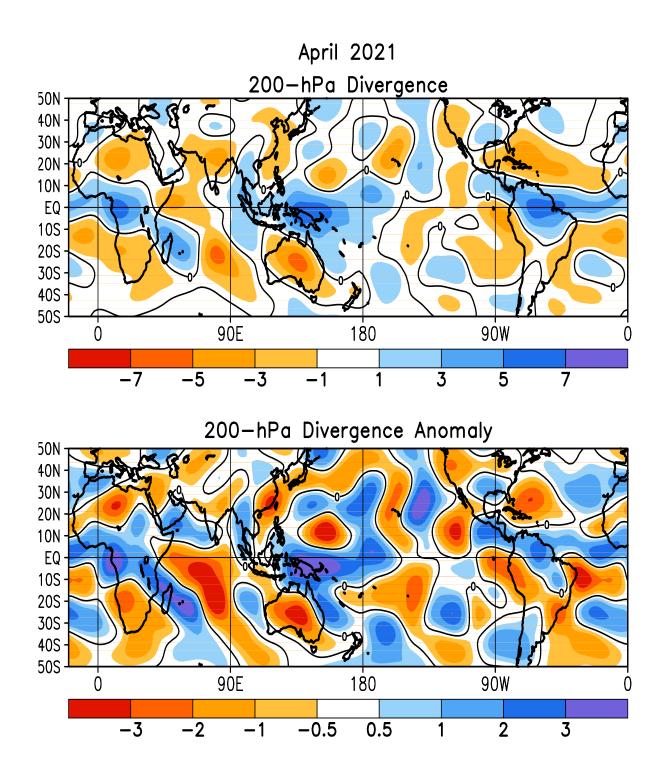

200-hPa Divergence Anomaly

FIGURE T23. Mean (top) and anomalous (bottom) 200-hPa divergence (CDAS/Reanalysis). Divergence and anomalous divergence are shaded blue. Convergence and anomalous convergence are shaded orange. Anomalies are departures from the 1981-2010 base period monthly means.
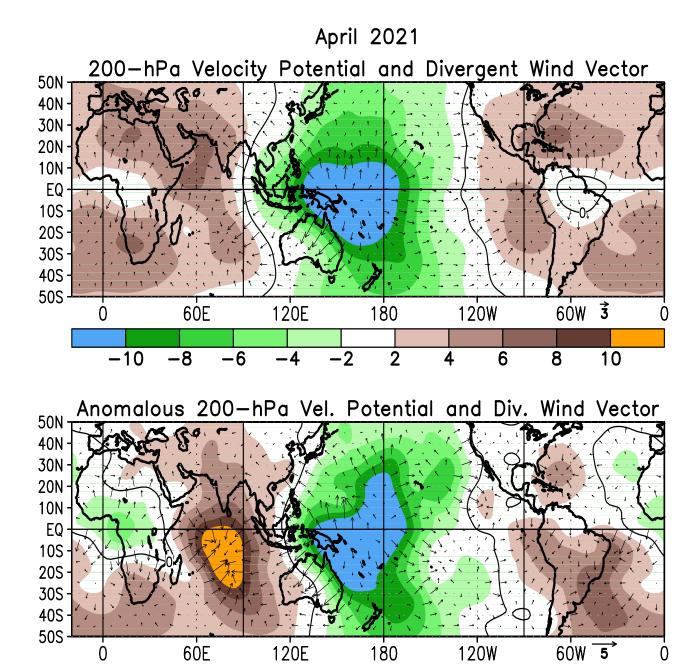
April 2021

200-hPa Velocity Potential and Divergent Wind Vector

Anomalous 200-hPa Vel. Potential and Div. Wind Vector

FIGURE T24. Mean (top) and anomalous (bottom) 200-hPa velocity potential ($10^6 m^2 s$) and divergent wind (CDAS/ Reanalysis). Anomalies are departures from the 1981-2010 base period monthly means.

April 2021

Outgoing Longwave Radiation (W/m2)
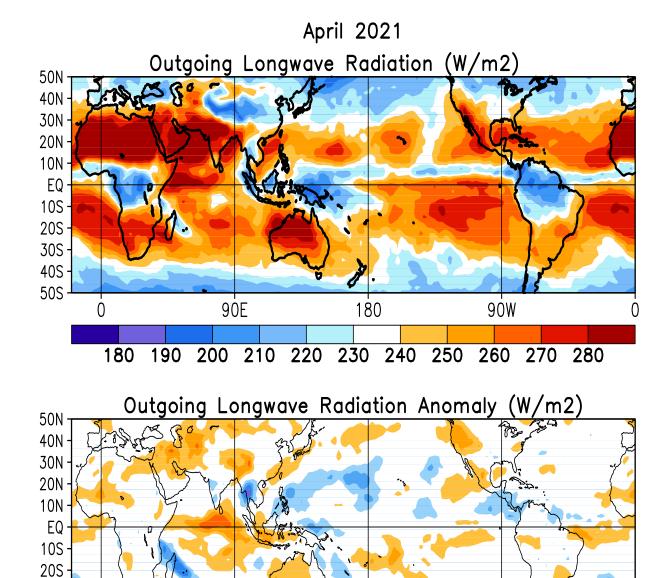

Outgoing Longwave Radiation Anomaly (W/m2)

FIGURE T25. Mean (top) and anomalous (bottom) outgoing longwave radiation for APR 2021 (NOAA 18 AVHRR IR window channel measurements by NESDIS/ORA). OLR contour interval is 20 Wm^{-2} with values greater than 280 Wm^{-2} indicated by dashed contours. Anomaly contour interval is 15 Wm^{-2} with positive values indicated by dashed contours and light shading. Anomalies are departures from the 1981-2010 base period monthly means.

April 2021

SSM/I Estimated Precipitation (mm)
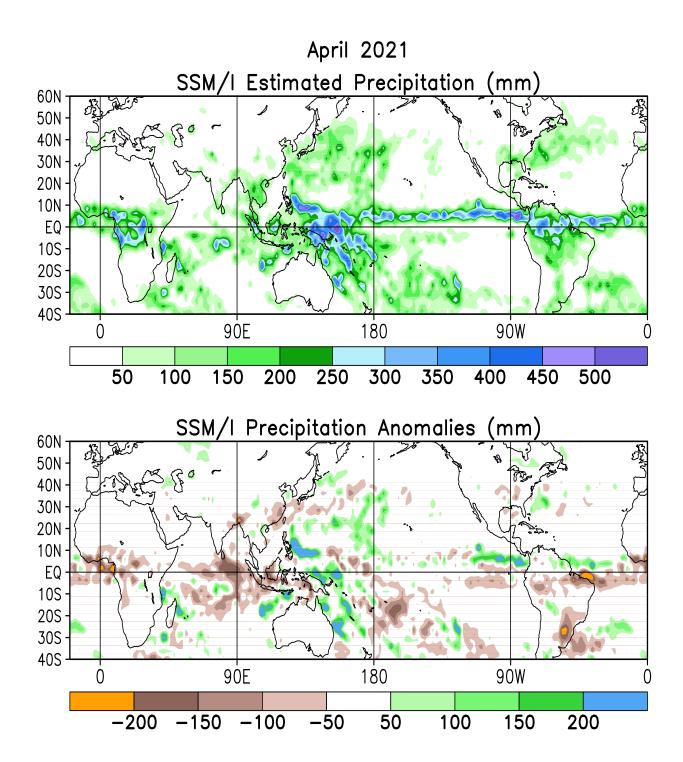

SSM/I Precipitation Anomalies (mm)

FIGURE T26. Estimated total (top) and anomalous (bottom) rainfall (mm) based on the Special Sensor Microwave/ Imager (SSM/S) precipitation index (Ferraro 1997, *J. Geophys. Res.,* **102**, 16715-16735). Anomalies are computed from the SSM/I 1987-2010 base period monthly means. Anomalies have been smoothed for display purposes.
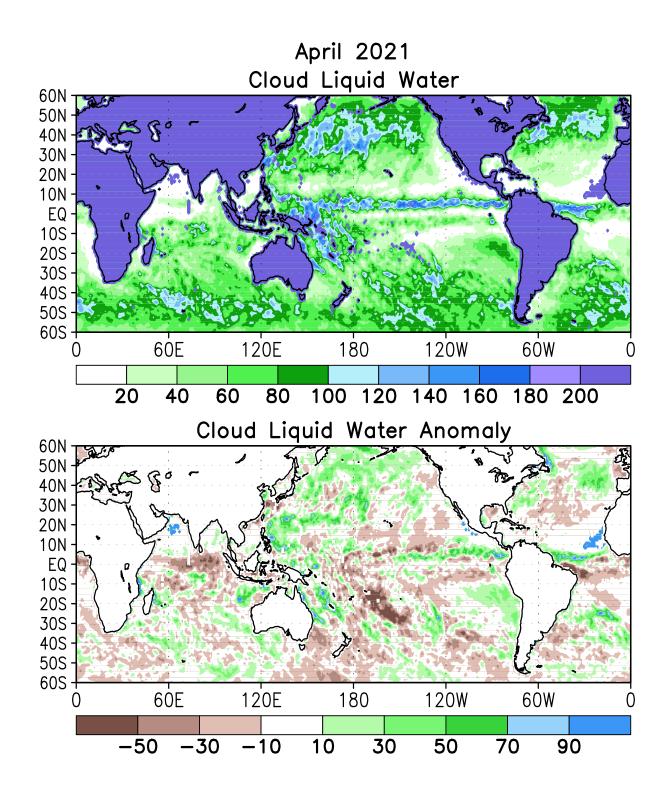
April 2021
Cloud Liquid Water

Cloud Liquid Water Anomaly

FIGURE T27. Mean (top) and anomalous (bottom) cloud liquid water (g m^{-2}) based on the Special Sensor Microwave/ Imager (SSM/I) (Weng et al 1997: *J. Climate*, **10**, 1086-1098). Anomalies are calculated from the 1987-2010 base period means.
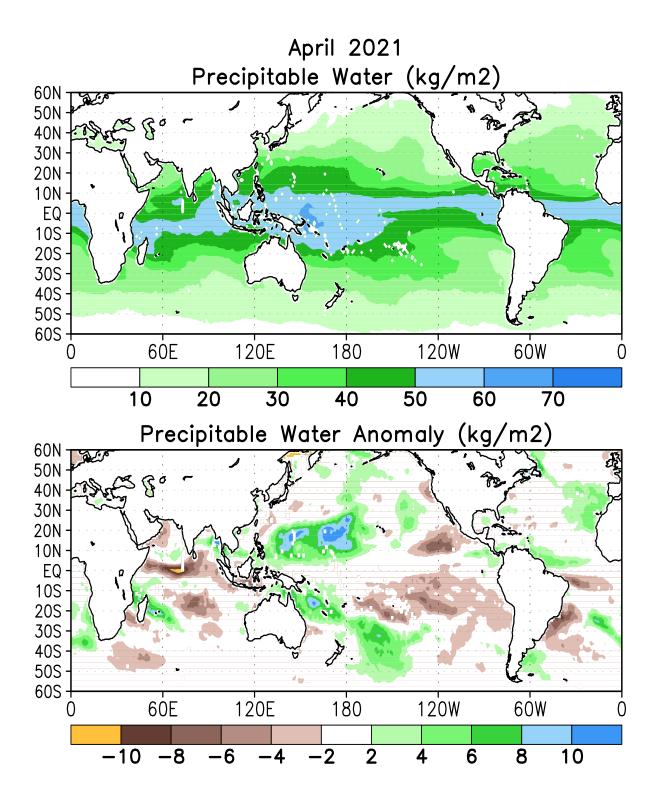
FIGURE T28. Mean (top) and anomalous (bottom) vertically integrated water vapor or precipitable water (kg m^{-2}) based on the Special Sensor Microwave/Imager (SSM/I) (Ferraro et. al, 1996: *Bull. Amer. Meteor. Soc.,* **77**, 891-905). Anomalies are calculated from the 1987-2010 base period means.
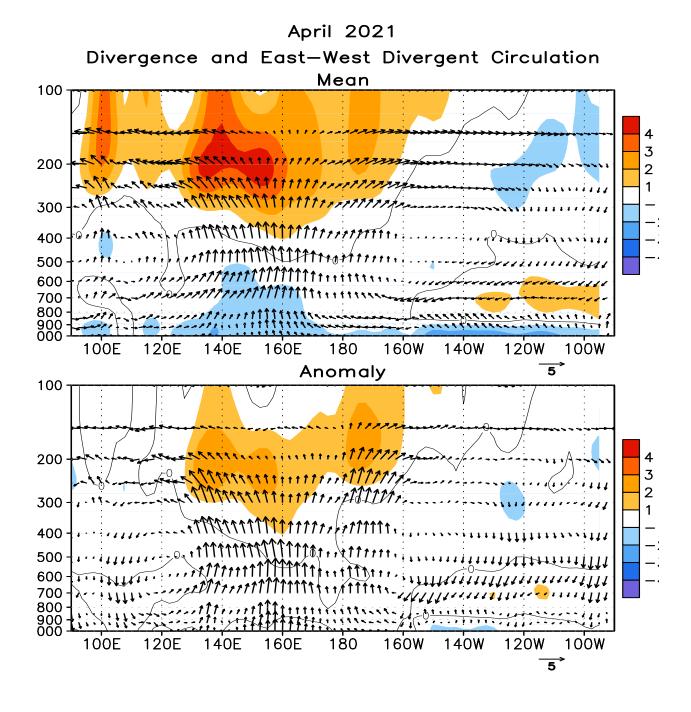
FIGURE T29. Pressure-longitude section (100E-80W) of the mean (top) and anomalous (bottom) divergence (contour interval is 1 x 10^{-6} s^{-1}) and divergent circulation averaged between 5N-5S. The divergent circulation is represented by vectors of combined pressure vertical velocity and the divergent component of the zonal wind. Red shading and solid contours denote divergence (top) and anomalous divergence (bottom). Blue shading and dashed contours denote convergence (top) and anomalous convergence (bottom). Anomalies are departures from the 1981-2010 base period monthly means.
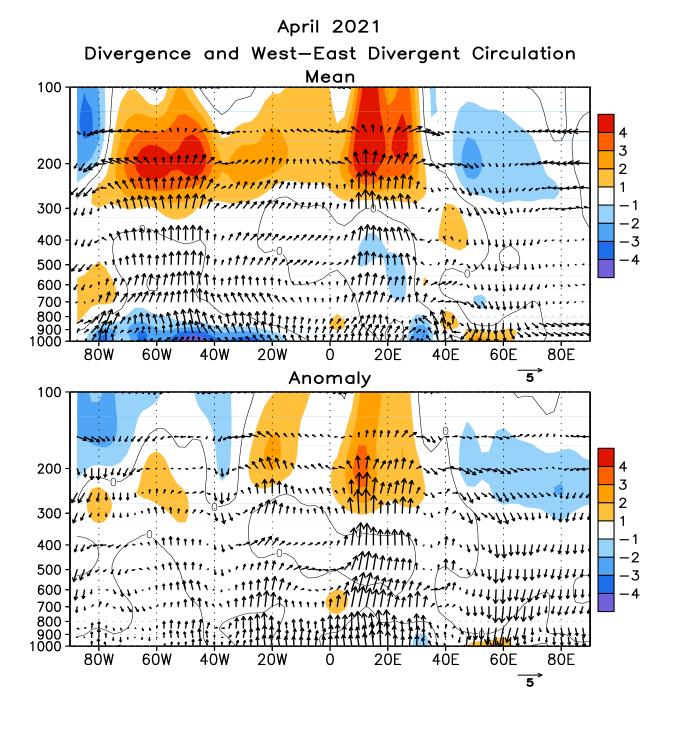
FIGURE T30. Pressure-longitude section (80W-100E) of the mean (top) and anomalous (bottom) divergence (contour interval is 1 x 10⁻⁶ s⁻¹) and divergent circulation averaged between 5N-5S. The divergent circulation is represented by vectors of combined pressure vertical velocity and the divergent component of the zonal wind. Red shading and solid contours denote divergence (top) and anomalous divergence (bottom). Blue shading and dashed contours denote convergence (top) and anomalous convergence (bottom). Anomalies are departures from the 1981-2010 base period monthly means.
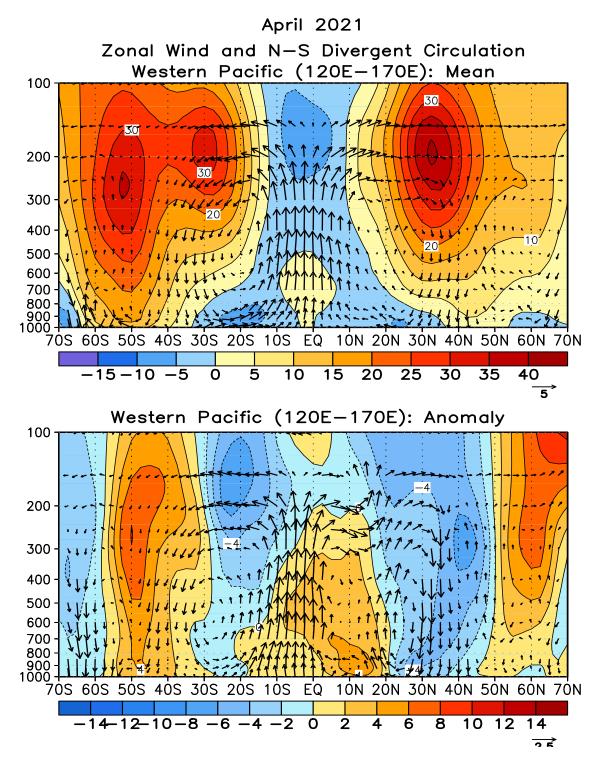
FIGURE T31. Pressure-latitude section of the mean (top) and anomalous (bottom) zonal wind (m s^{-1}) and divergent circulation averaged over the west Pacific sector (120E-170E). The divergent circulation is represented by vectors of combined pressure vertical velocity and the divergent component of the meridional wind. Red shading and solid contours denote a westerly (top) or anomalous westerly (bottom) zonal wind. Blue shading and dashed contours denote an easterly (top) or anomalous easterly (bottom) zonal wind. Anomalies are departures from the 1981-2010 base period monthly means.
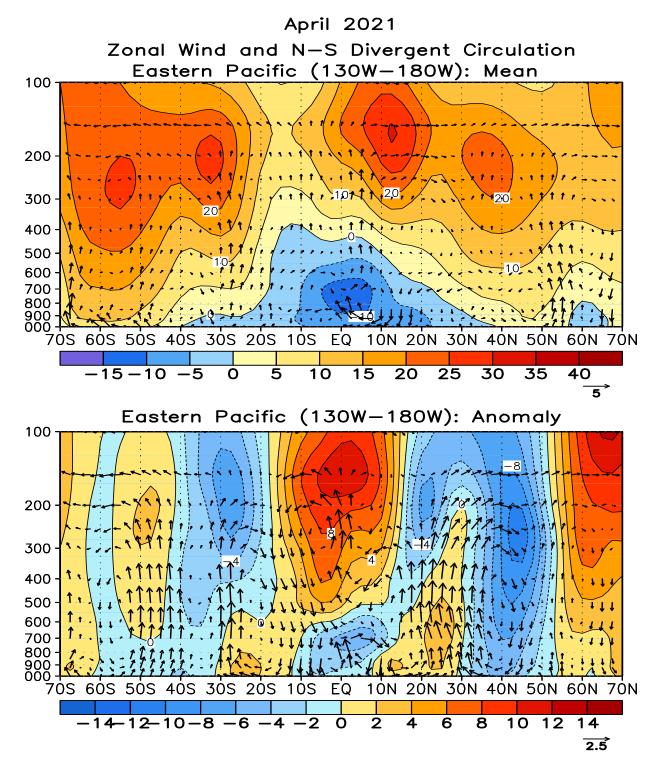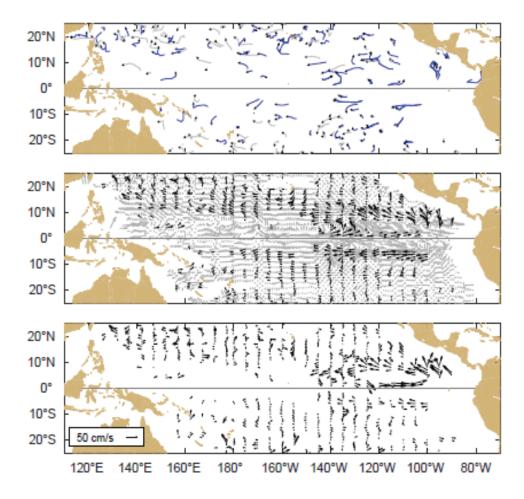
FIGURE T32. Pressure-latitude section of the mean (top) and anomalous (bottom) zonal wind (m s⁻¹) and divergent circulation averaged over the central Pacific sector (130W-180W). The divergent circulation is represented by vectors of combined pressure vertical velocity and the divergent component of the meridional wind. Red shading and solid contours denote a westerly (top) or anomalous westerly (bottom) zonal wind. Blue shading and dashed contours denote an easterly (top) or anomalous easterly (bottom) zonal wind. Anomalies are departures from the 1981-2010 base period monthly means.

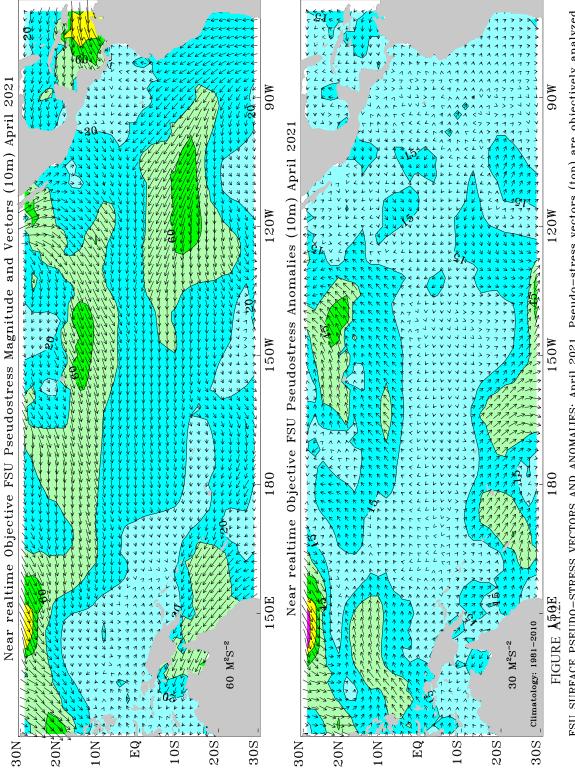Tropical Pacific Drifting Buoys   R. Lumpkin/M. Pazos, AOML, Miami

During April 2021, 213 satellite-tracked surface drifting buoys were reporting from the tropical Pacific. The drifters did not reveal large-scale anomalies from April surface current climatology; large eastward anomalies measured by a small number of near-equatorial drifters at 110W may have been associated with a Tropical Instability Wave.
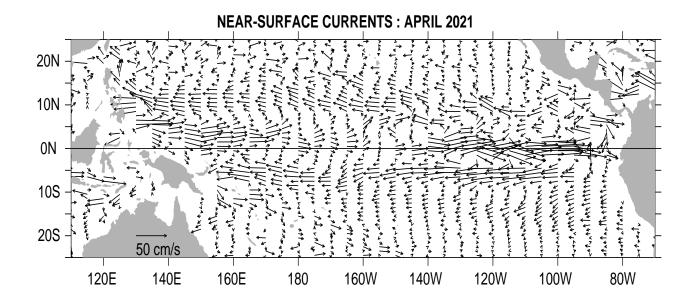

Figure A1.1 Top: Movements of drifting buoys in the tropical Pacific Ocean during April 2021. The linear segments of each trajectory represent a one week displacement. Trajectories of buoys which have lost their subsurface drogues are gray; those with drogues are black.
Middle: Monthly mean currents calculated from all buoys 1993-2002 (gray), and currents measured by the drogued buoys this month (black) smoothed by an optimal filter.
Bottom: Anomalies from the climatological monthly mean currents for this month.

Near realtime Objective FSU Pseudostress Magnitude and Vectors (10m) April 2021

Near realtime Objective FSU Pseudostress Anomalies (10m) April 2021

FIGURE A.20.

NEAR-SURFACE CURRENTS : APRIL 2021

APRIL 2021 ANOMALIES

FIGURE A1.3. Ocean Surface Current Analysis-Real-time (OSCAR) for APR 2021 (Bonjean and Lagerloef 2002, J. Phys. Oceanogr., Vol. 32, No. 10, 2938-2954; Lagerloef et al. 1999, JGR-Oceans, 104, 23313-23326). (top) Total velocity. Surface currents are calculated from satellite data including Jason sea level anomalies and NCEP winds. (bottom) Velocity anomalies. The subtracted climatology was based on SSM/I and QuickScat winds and Topex/ Poseidon and Jason from 1993-2003. See also http://www.oscar.noaa.gov.

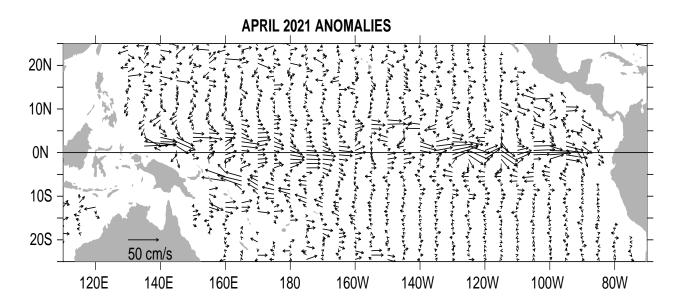**NEAR-SURFACE CURRENTS : APRIL 2021**
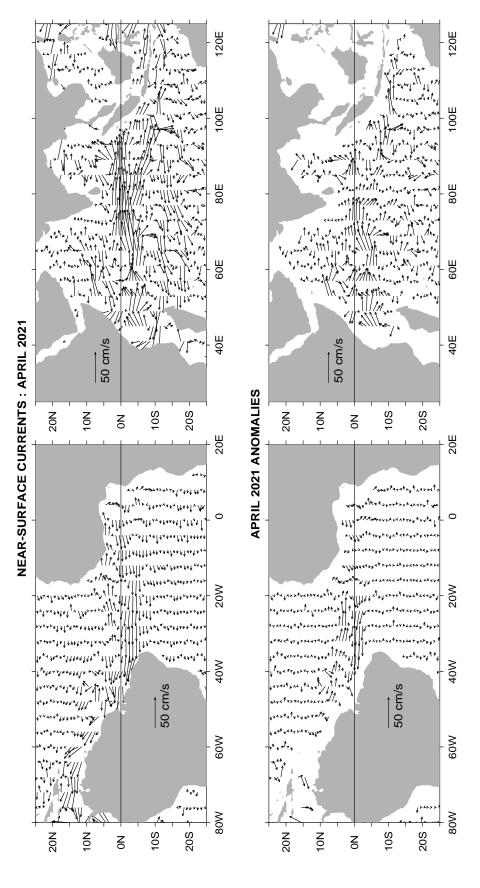
APRIL 2021 ANOMALIES

FIGURE A1.4. Ocean Surface Current Analysis-Real-time (OSCAR) for APR 2021 (Bonjean and Lagerloef 2002, J. Phys. Oceanogr., Vol. 32, No. 10, 2938-2954; Lagerloef et al. 1999, JGR-Oceans, 104, 23313-23326). (top) Total velocity. Surface currents are calculated from satellite data including Jason sea level anomalies and NCEP winds. (bottom) Velocity anomalies. The subtracted climatology was based on SSM/I and QuickScat winds and Topex/Poseidon and Jason from 1993-2003. See also http://www.oscar.noaa.gov.

44

Forecast Forum

The canonical correlation analysis (CCA) forecast of SST in the central Pacific (Barnett et al. 1988, *Science*, **241**, 192196; Barnston and Ropelewski 1992, *J. Climate*, **5**, 13161345), is shown in **Figs. F1 and F2.** This forecast is produced routinely by the Prediction Branch of the Climate Prediction Center. The predictions from the National Centers for Environmental Prediction (NCEP) Coupled Forecast System Model (CFS03) are presented in **Figs. F3 and F4a, F4b**. Predictions from the Markov model (Xue, et al. 2000: *J. Climate*, **13**, 849871) are shown in **Figs. F5 and F6.** Predictions from the latest version of the LDEO model (Chen et al. 2000: *Geophys. Res. Let.*, **27**, 25852587) are shown in **Figs. F7 and F8**. Predictions from the ENSO CLIPER statistical model (Knaff and Landsea 1997, Wea. Forecasting, 12, 633 652) are shown in **Fig. F9**. Niño 3.4 predictions are summarized in **Fig. F10**, provided by the Forecasting and Prediction Research Group of the IRI.

The CPC and the contributors to the **Forecast Forum** caution potential users of this predictive information that they can expect only modest skill.

ENSO Alert System Status: Final La Niña Advisory

Outlook

La Niña has ended, with ENSO-neutral likely to continue through the Northern Hemisphere summer (67% chance in June-August 2021).

Discussion

During April, the tropical Pacific Ocean returned to ENSO-neutral conditions as the coupling between the atmosphere and ocean weakened. Sea surface temperatures were near-to-below average across most of the equatorial Pacific Ocean in the past month (Fig. T18). The Niño indices have generally trended toward normal during the last several months, except for the easternmost Niño-1+2 region, which was -0.8ºC in the past month (Table T2). Subsurface temperature anomalies continued to increase due to a downwelling Kelvin wave, which reinforced the positive temperature anomalies along the thermocline (Fig. T17). Low-level easterly wind anomalies were weakly present in the east-central Pacific, but were westerly in the far western Pacific Ocean (Fig. T20), while upper-level wind anomalies remained westerly across the central and east-central tropical Pacific (Fig. T21). Tropical convection became near average around the Date Line in the past month, with suppressed convection evident over Indonesia (Fig. T25). Overall, the ocean and atmosphere system reflected a return to ENSO-neutral.

Most of the models in the IRI/CPC plume predict a continuation of ENSO-neutral through the Northern Hemisphere summer 2021 (Figs. F1-F12). The forecaster consensus agrees with this set of models through the summer, and then begins hedging toward cooler conditions as the Northern

Hemisphere fall approaches. La Niña chances are around 50-55% during the late fall and winter, which is in alignment with forecasts from the NCEP Climate Forecast System and North American Multi-model Ensemble. However, there is typically large uncertainty with forecasts made in the spring, so confidence in ENSO-neutral for the coming seasons is highest. In summary, La Niña has ended, with ENSO-neutral likely to continue through the Northern Hemisphere summer (67% chance in June-August 2021).

.

Weekly updates of oceanic and atmospheric conditions are available on the Climate Prediction Center homepage (El Niño/La Niña Current Conditions and Expert Discussions).
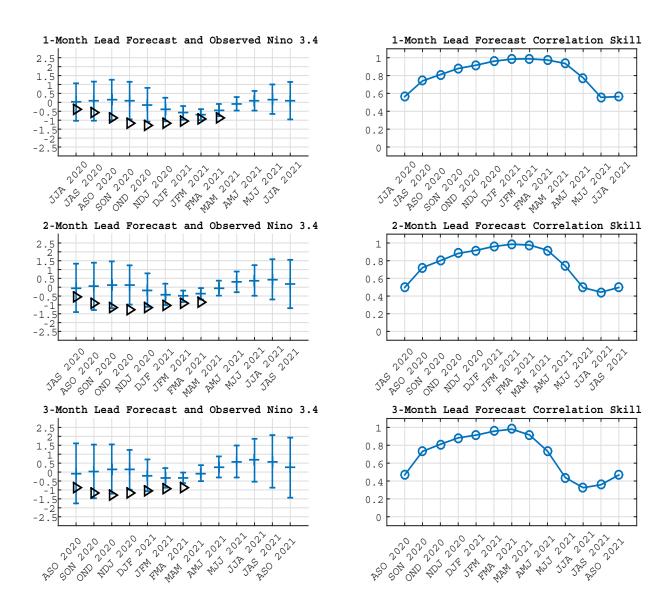
FIGURE F1. Canonical correlation analysis (CCA) sea surface temperature (SST) anomaly prediction for the central Pacific (5N to 5S, 120W to 170W (Barnston and Ropelewski, 1992,i J. Climate, 5, 1316-1345)). The three plots on the left are, from top to bottom, the 1-month, 2-month, and 3-month lead seasonal forecasts from the past 12 months plus the current month. The triangles in each plot are the observed SST anomaly through the latest available season. The lines at the mid-points of the forecast error bars represent the real-time CCA predictions based on the anomalies of quasi-global sea level pressure, the anomalies of tropical Pacific SST, and heat content of the upper 300 meters of the near-equator tropical Pacific (10S to 10N). The vertical lines represent the two standard deviation error bars for the predictions based on past performance. The three plots on the right are skill values for the corresponding seasons, from the correlations of the predicted and observed SST in the prior 10 years of simulated real-time forecasts. Skill values show a clear annual cycle and are inversely proportional to the length of the error bars depicted in the forecast time series.

47

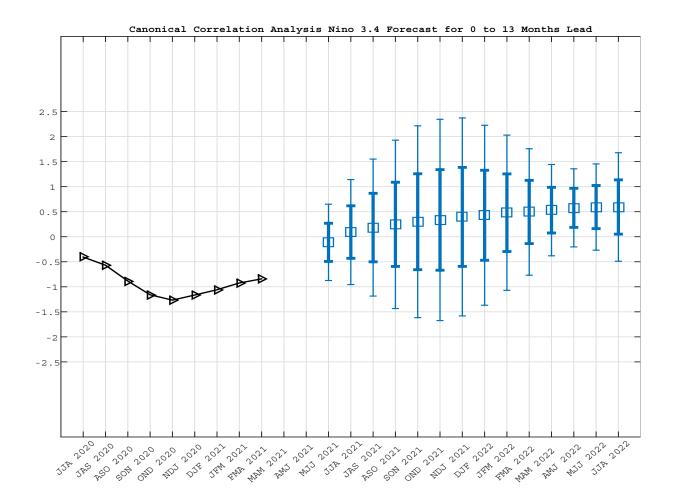**Canonical Correlation Analysis Nino 3.4 Forecast for 0 to 13 Months Lead**

FIGURE F2. Canonical Correlation Analysis (CCA) forecast of sea-surface temperature anomalies for the Nino 3.4 region (5N-5S, 120W-170W) for the upcoming year of three-month overlapping periods. The CCA predictions are based on anomaly patterns of sea level pressure, tropical Pacific SST, and heat content of the upper 300 meters of the near-equator tropical Pacific (10S to 10N). Small squares at the midpoints of the vertical forecast bars represent the CCA predictions, and the bars show the one (thick) and two (thin) standard deviation errors. The triangles and line represent the observed three-month mean SST anomaly in the Nino 3.4 region up to the most recently available data.
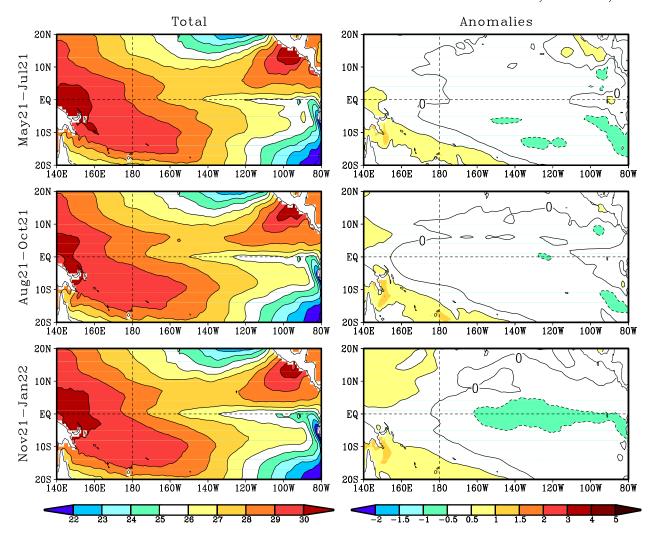
FIGURE F3. Predicted 3-month average sea surface temperature (left) and anomalies (right) from the NCEP Coupled Forecast System Model (CFS03). The forecasts consist of 40 forecast members. Contour interval is 1°C, with additional contours for 0.5°C and -0.5°C. Negative anomalies are indicated by dashed contours.

Forecast Nino3 SST anomalies from CFSv2
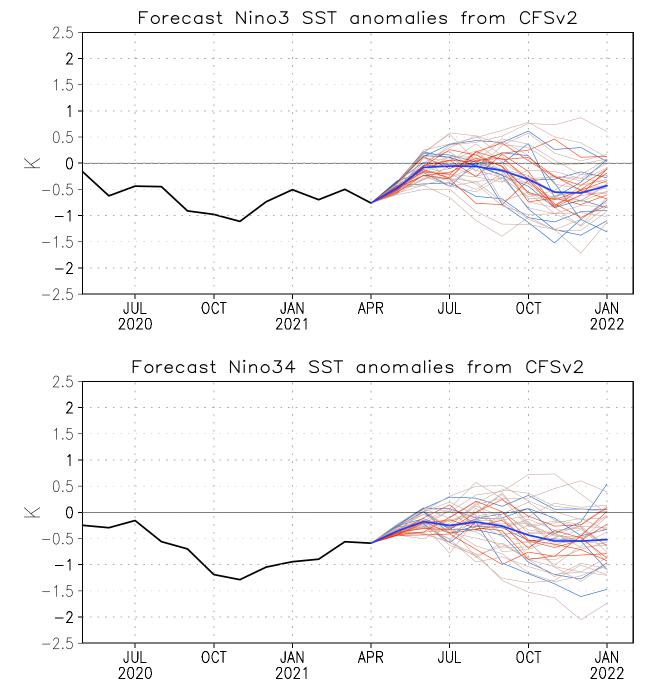

Forecast Nino34 SST anomalies from CFSv2

FIGURE F4.   Predicted and observed sea surface temperature (SST) anomalies for the Nino 3 (top) and Nino 3.4
(bottom) regions from the NCEP Coupled Forecast System Model (CFS03). The forecasts consist of 40 forecast
members. The ensemble mean of all 40 forecast members is shown by the blue line, individual members are shown
by thin lines, and the observation is indicated by the black line. The Nino-3 region spans the eastern equatorial
Pacific between 5N-5S, 150W-90W. The Nno 3.4 region spans the east-central equatorial Pacific between 5N-5S,
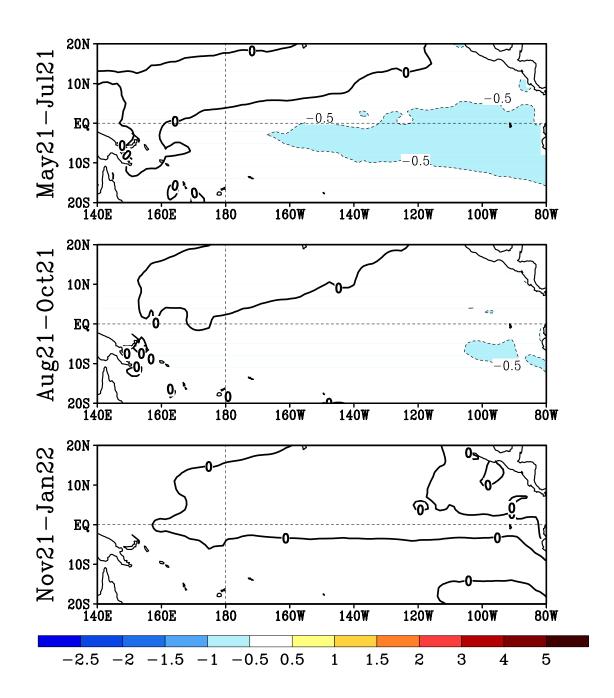170W-120W.

FIGURE F5. Predicted 3-month average sea surface temperature anomalies from the NCEP/CPC Markov model (Xue et al. 2000, *J. Climate*, **13**, 849-871). The forecast is initiated in APR 2021 . Contour interval is 0.3C and negative anomalies are indicated by dashed contours. Anomalies are calculated relative to the 1971-2000 climatology.
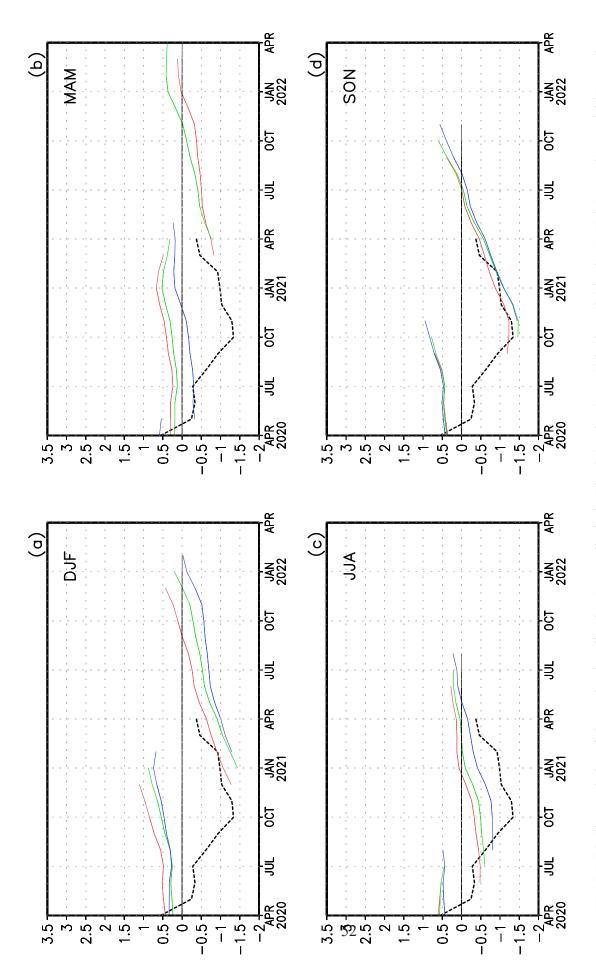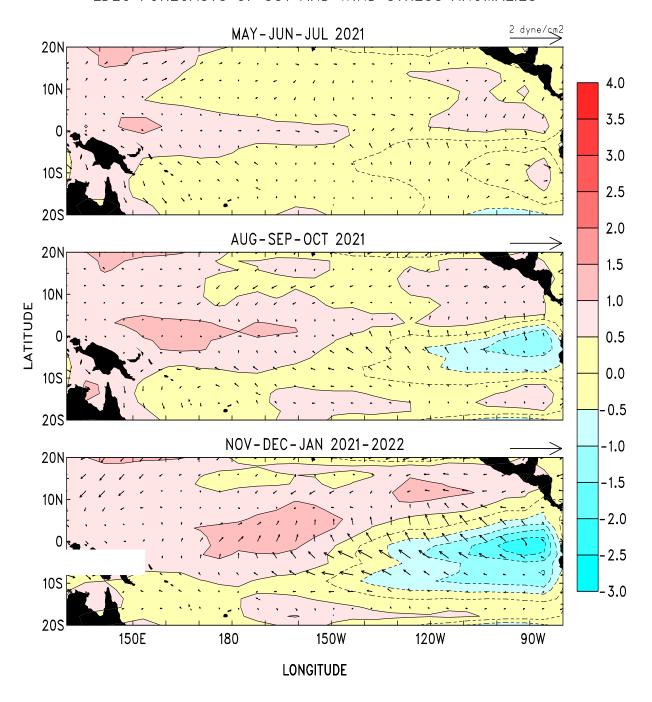
FIGURE F6. Time evolution of observed and predicted SST anomalies in the Nino 3.4 region (up to 12 lead months) by the NCEP/CPC Markov model (Xue et al. 2000, *J. Climate*, **13**, 849-871). Anomalies are calculated relative to the 1971-2000 climatology. Shown in each panel are the forecasts grouped by three consecutive starting months: (a) is for December, January, and February, (b) is for March, April, and May, (c) is for June, July, and August, and (d) is for September, October, and November. The observed Nino 3.4 SST anomalies are indicated by the black dashed lines. The Nino 3.4 region spans the east-central equatorial Pacific between 5N-5S, 170W-120W.

FIGURE F7. Forecasts of the tropical Pacific Predicted SST (shading) and vector wind anomalies for the next 3 seasons based on the LDEO model. Each forecast represents an ensemble average of 3 sets of predictions initialized during the last three consecutive months (see Figure F8).

LDEO FORECASTS OF NINO3

FIGURE F8. LDEO forecasts of SST anomalies for the Nino 3 region using wind stresses obtained from (top) Qui-kSCAT, (middle) NCEP, and (bottom) Florida State Univ. (FSU), along with SSTs (obtained from NCEP), and sea surface height data (obtained from TOPEX/POSEIDON) data. Each thin blue line represents a 12-month forecast, initialized one month apart for the past 24 months. Observed SST anomalies are indicated by the thick red line. The Nino-3 region spans the eastern equatorial Pacific between 5N-5S, 150W-90W.
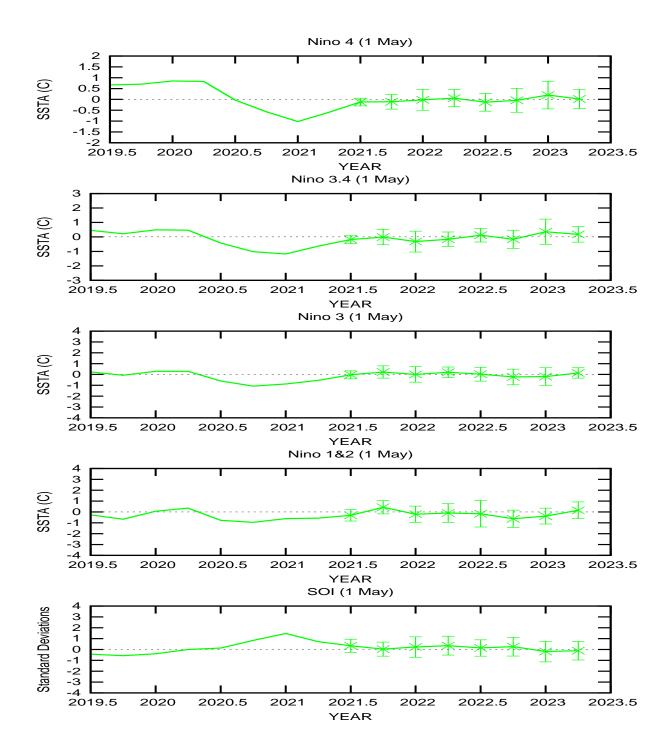
FIGURE F9. ENSO-CLIPER statistical model forecasts of three-month average sea surface temperature anomalies (green lines, deg. C) in (top panel) the Nino 4 region (5N-5S, 160E-150W), (second panel) the Nino 3.4 region (5N-5S, 170W-120W), (third panel) the Nino 3 region (5N-5S, 150W-90W), and (fourth panel) the Nino 1+2 region (0-10S, 90W-80W) (Knaff and Landsea 1997, *Wea. Forecasting*, **12**, 633-652). Bottom panel shows predictions of the three-month standardized Southern Oscillation Index (SOI, green line). Horizontal bars on green line indicate the adjusted root mean square error (RMSE). The Observed three-month average values are indicated by the thick blue line. SST anomalies are departures from the 1981-2010 base period means, and the SOI is calculated from the 1951-1980 base period means.
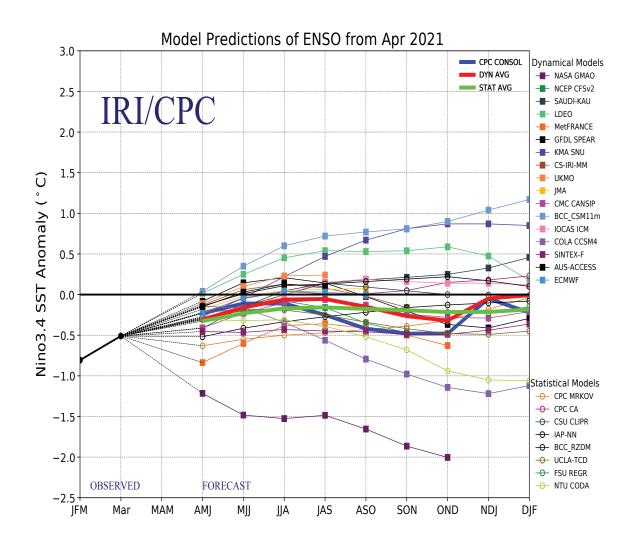
55

FIGURE F10. Time series of predicted sea surface temperature anomalies for the Nino 3.4 region (deg. C) from various dynamical and statistical models for nine overlapping 3-month periods. The Nino 3.4 region spans the east-central equatorial Pacific between 5N-5S, 170W-120W. Figure provided by the International Research Institute (IRI).

Extratropical Highlights – April 2021

1. Northern Hemisphere

The 500-hPa circulation during April featured above-average heights over northern Siberia, Greenland and surrounding seas and The North Pacific Ocean, and below-average heights over the North Atlantic Ocean, the Arctic Ocean, Scandinavia, and central Canada (Fig. E9).

The main land-surface temperature signals included above-average temperatures in eastern Canada, southwestern and west-coastal states of the continental U.S., northwestern portions of Russia, the Middle East, and western portions of North Africa (Fig. E1). The main precipitation signals included above-average totals in the southeastern U.S., eastern portions of Canada, western, central, and eastern portions of Russia, and below-average totals in the northwest and midwest regions of the U.S., the British Isles, and western Europe (Fig. E3).

a. North America

The 500-hPa circulation during April featured above-average heights over eastern portions of Canada, The Gulf of Alaska, and along the west coast of the continental U.S. (Fig. E9). Despite these circulation anomalies, much of the continental U.S. and Alaska had near normal temperatures on average for April. The west coast states, southwest states, Great Lakes region, and New England had moderately above-average temperatures, with percentiles between the 70th and 90th percent of occurrence (Fig. E1). The circulation pattern off the Gulf of Alaska contributed to below-average precipitation in the northwest states of the U.S., resulting in dry conditions at the 10th percentile of occurrence (Fig. E3). The U.S. Drought Monitor for May also indicates no change in the "abnormal" to "extreme" dry conditions there, with some degradation in status for eastern portions of Oregon. Departures from normal precipitation accumulation for April are on the order of 50-150mm below normal for the combined areas of western Washington, Oregon and Northern California (Fig. E6) Meanwhile, the Mississippi Valley had much above-average rainfall with departures from normal at 150mm or more for the Mississippi Delta area (Figs. E3 and E6). According to the U.S. Drought Monitor for May, the continued restoration of soil moisture levels in the southeastern U.S. has led to Class 2 and 3 Improvements for the region.

b. Greenland, Europe and Scandinavia

The 500-hPa height pattern during April featured a high-amplitude ridge over the British Isles that stretched across the Norweigian Sea to Greenland (Fig. E9). Temperature anomalies were only slightly above-normal for April (Fig. E1), however total rainfall was below-average with totals less than 100mm resulting in a low-percentile (10th) for April (Figs. E3 and E4).

2. Southern Hemisphere

The 500-hPa height field during April featured above-average heights in the central South Pacific and Indian Oceans, with highest departures from normal over the South Atlantic Ocean. Below-average heights are primarily in sections of the Southern Ocean and an adjacent area in the eastern portions of the South Pacific Ocean (Fig. E15). Southeastern portions of South America saw below-average precipitation with totals in the 10th percentile while northeastern Australia had above-average precipitation in the 80th percentile or better (Fig. E4). In southern Africa, the monsoon season runs from October to April. During April, rainfall was near normal for most of the area with some areas below-average for the 2020-2021 season (Fig. E3).

TELECONNECTION INDICES

Month	North Atlantic			North Pacific			EURASIA		
	NAO	EA	WP	EP-NP	PNA	TNH	EATL/WRUS	SCAND	POLEUR
APR 21	-1.7	0.3	-0.1	0.8	-1.3	---	-0.4	-1.2	-0.2
MAR 21	0.4	-0.2	2.1	-1.3	-1.2	---	3.0	-0.9	0.6
FEB 21	-0.3	1.2	0.8	-0.8	-0.7	1.3	0.8	0.3	-3.2
JAN 21	-1.8	-0.0	2.5	-0.7	-0.4	-0.1	-1.3	0.3	-1.6
DEC 20	-0.4	-0.8	1.0	---	1.3	0.2	-1.1	2.3	0.1
NOV 20	2.5	0.0	0.7	-0.7	0.2	---	0.1	-0.1	-0.6
OCT 20	-0.2	-0.2	-1.2	0.6	-1.1	---	-1.8	1.5	-1.0
SEP 20	1.1	1.9	-2.4	0.1	0.6	---	-0.9	-0.5	0.3
AUG 20	0.0	1.6	-0.2	-2.4	1.8	---	0.6	-1.6	-0.5
JUL 20	-1.2	0.5	-0.5	-2.0	1.2	---	-0.7	-2.3	-0.1
JUN 20	0.2	-0.1	-1.2	-0.7	0.9	---	-2.0	0.6	-0.2
MAY 20	-0.3	0.1	0.1	0.0	0.3	---	-0.5	-2.4	-1.1
APR 20	-1.3	0.6	-1.3	1.5	-1.4	---	1.8	-1.5	0.4

TABLE E1–Standardized amplitudes of selected Northern Hemisphere teleconnection patterns for the most recent thirteen months (computational procedures are described in Fig. E7). Pattern names and abbreviations are North Atlantic Oscillation (NAO); East Atlantic pattern (EA); West Pacific pattern (WP); East Pacific - North Pacific pattern (EP-NP); Pacific/North American pattern (PNA); Tropical/Northern Hemisphere pattern (TNH); East Atlantic/Western Russia pattern (EATL/WRUS-called Eurasia-2 pattern by Barnston and Livezey, 1987, *Mon. Wea. Rev.*, **115**, 1083-1126); Scandanavia pattern (SCAND-called Eurasia-1 pattern by Barnston and Livezey 1987); and Polar Eurasia pattern (POLEUR). No value is plotted for calendar months in which the pattern does not appear as a leading mode.

April 2021
Temperature Anomalies (C)

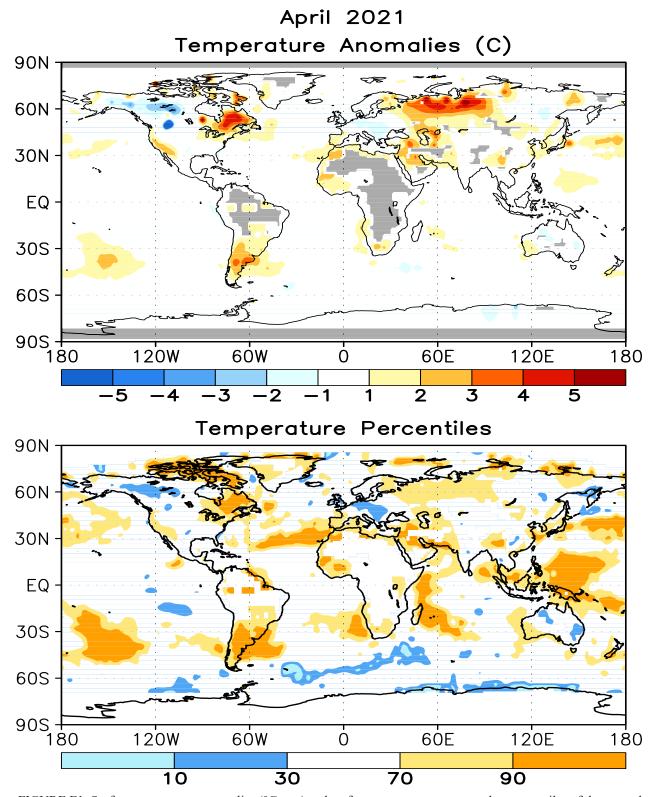
Temperature Percentiles

FIGURE E1. Surface temperature anomalies (°C, top) and surface temperature expressed as percentiles of the normal (Gaussian) distribution fit to the 1981–2010 base period data (bottom) for APR 2021. Analysis is based on station data over land and on SST data over the oceans (top). Anomalies for station data are departures from the 1981–2010 base period means, while SST anomalies are departures from the 1981–2010 adjusted OI climatology. (Smith and Reynolds 1998, *J. Climate*, **11**, 3320-3323). Regions with insufficient data for analysis in both figures are indicated by shading in the top figure only.

FIGURE E2. Monthly global (top), Northern Hemisphere (middle), and Southern Hemisphere (bottom) surface temperature anomalies (land only, °C) from January 1990 - present, computed as departures from the 1981–2010 base period means.

April 2021
Precipitation Anomalies (mm)

Precipitation Percentiles

FIGURE E3. Anomalous precipitation (mm, top) and precipitation percentiles based on a Gamma distribution fit to the 1981–2010 base period data (bottom) for APR 2021. Data are obtained from a merge of raingauge observations and satellite-derived precipitation estimates (Janowiak and Xie 1999, *J. Climate*, **12**, 3335–3342). Contours are drawn at 200, 100, 50, 25, -25, -50, -100, and -200 mm in top panel. Percentiles are not plotted in regions where mean monthly precipitation is <5mm/month.

FIGURE E4. Areal estimates of monthly mean precipitation amounts (mm, solid lines) and precipitation percentiles (%, bars) for the most recent 13 months obtained from a merge of raingauge observations and satellite-derived precipitation estimates (Janowiak and Xie 1999, *J. Climate*, **12**, 3335–3342). The monthly precipitation climatology (mm, dashed lines) is from the 1981–2010 base period monthly means. Monthly percentiles are not shown if the monthly mean is less than 5 mm.
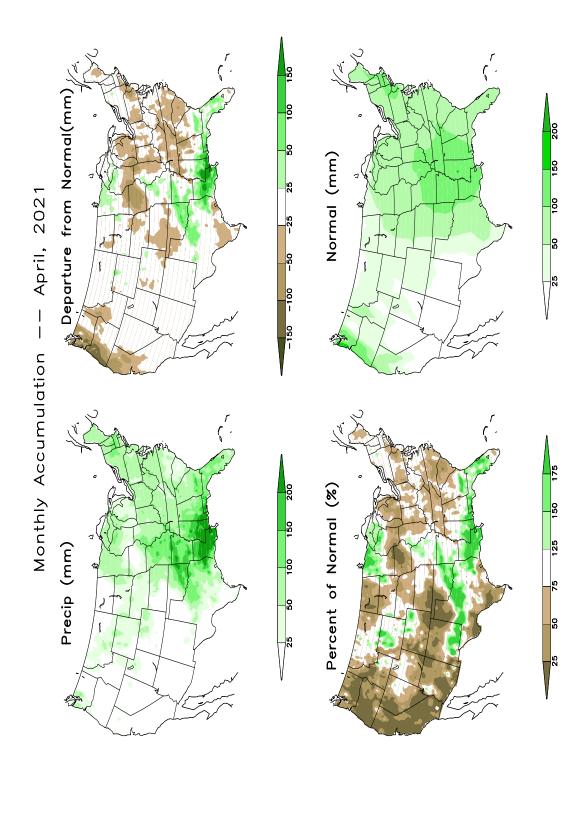
FIGURE E5. Areal estimates of monthly mean precipitation amounts (mm, solid lines) and precipitation percentiles (%, bars) for the most recent 13 months obtained from a merge of raingauge observations and satellite-derived precipitation estimates (Janowiak and Xie 1999, *J. Climate*, **12**, 3335–3342). The monthly precipitation climatology (mm, dashed lines) is from the 1981–2010 base period monthly means. Monthly percentiles are not shown if the monthly mean is less than 5 mm.

Monthly Accumulation -- April, 2021

FIGURE E6. Observed precipitation (upper left), departure from average (upper right), percent of average (lower left), and average precipitation (lower right) for APR 2021. The units are given on each panel. Base period for averages is 1981–2010. Results are based on CPC's U. S. daily precipitation analysis, which is available at   http://www.cpc.ncep.noaa.gov/prodcuts/precip/realtime.

FIGURE E7. Standardized monthly Northern Hemisphere teleconnection indices. The teleconnection patterns are calculated from a Rotated Principal Component Analysis (RPCA) applied to monthly standardized 500-hPa height anomalies during the 1981-2010 base period. To obtain these patterns, ten leading un-rotated modes are first calculated for each calendar month by using the monthly height anomaly fields for the three-month period centered on that month: [i.e., The July modes are calculated from the June, July, and August standardized monthly anomalies]. A Varimax spatial rotation of the ten leading un-rotated modes for each calendar month results in 120 rotated modes (12 months x 10 modes per month) that yield ten primary teleconnection patterns.The teleconnection indices are calculated by first projecting the standardized monthly anomalies onto the teleconnection patterns corresponding to that month (eight or nine teleconnection patterns are seen in each calendar month). The indices are then solved for simultaneously using a Least-Squares approach. In this approach, the indices are the solution to the Least-Squares system of equations which explains the maximum spatial structure of the observed height anomaly field during the month. The indices are then standardized for each pattern and calendar month independently. No index value exists when the teleconnection pattern does not appear as one of the ten leading rotated EOF's valid for that month.

FIGURE E8. Northern Hemisphere mean and anomalous sea level pressure (CDAS/Reanalysis) for APR 2021. Mean values are denoted by solid contours drawn at an interval of 4 hPa. Anomaly contour interval is 2 hPa with values less (greater) than -2 hPa (2 hPa) indicated by dark (light) shading. Anomalies are calculated as departures from the 1981-2010 base period monthly means.
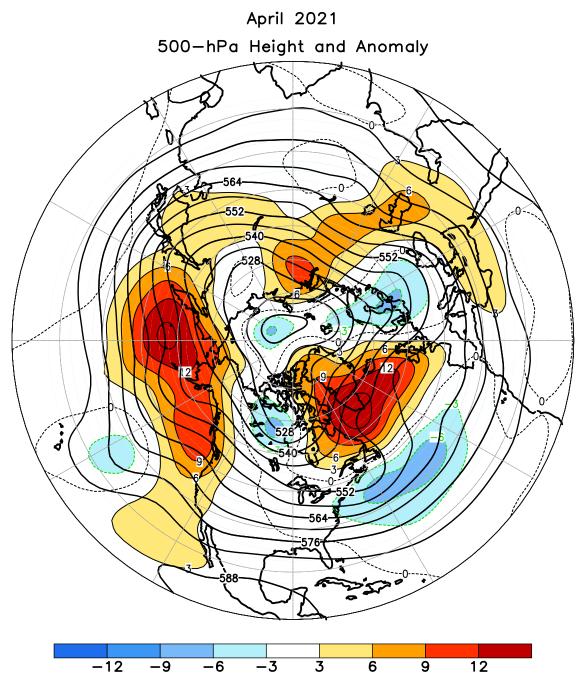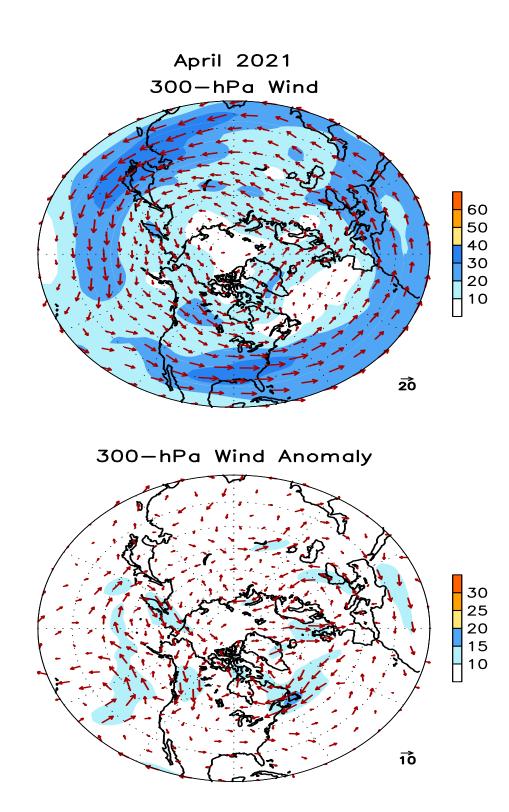
FIGURE E9. Northern Hemisphere mean and anomalous 500-hPa geopotential height (CDAS/Reanalysis) for APR 2021. Mean heights are denoted by solid contours drawn at an interval of 6 dam. Anomaly contour interval is 3 dam with values less (greater) than -3 dam (3 dam) indicated by dark (light) shading. Anomalies are calculated as departures from the 1981-2010 base period monthly means.

FIGURE E10. Northern Hemisphere mean (left) and anomalous (right) 300-hPa vector wind (CDAS/Reanalysis) for APR 2021. Mean (anomaly) isotach contour interval is 10 (5) ms^{-1}. Values greater than 30 ms^{-1} (left) and 10 ms^{-1} (rights) are shaded. Anomalies are departures from the 1981-2010 base period monthly means.

April 2021
500−hPa: Percentage of Anomaly Days

FIGURE E11. Northern Hemisphere percentage of days during APR 2021 in which 500-hPa height anomalies greater than 15 m (red) and less than -15 m (blue) were observed. Values greater than 70% are shaded and contour in-

FIGURE E12. Northern Hemisphere: Daily 500-hPa height anomalies for APR 2021 averaged over the 5° latitude band centered on 40°N. Positive values are indicated by solid contours and dark shading. Negative values are indicated by dashed coutours and light shading. Contour interval is 60 m. Anomalies are departures from the 1981-2010 base period daily means.

April 2021
500—hPa Heights (Contours)
High Frequency Std. Dev. (Shading)

500—hPa Heights (Contours)
Normalized High Frequency Variance (Shading)

FIGURE E13. Northern Hemisphere 500-hPa heights (thick contours, interval is 6 dam) overlaid with (Top) Standard deviation of 10-day high-pass (HP) filtered height anomalies and (Bottom) Normalized anomalous variance of 10-day HP filtered height anomalies. A Lanczos filter is used to calculate the HP filtered anomalies. Anomalies are departures from the 1981-2010 daily means.

April 2021
Sea−Level Pressure and Anomaly

FIGURE E14. Southern Hemisphere mean and anomalous sea level pressure(CDAS/Reanalysis) for APR 2021. Mean values are denoted by solid contours drawn at an interval of 4 hPa. Anomaly contour interval is 2 hPa with values less (greater) than -2 hPa (2 hPa) indicated by dark (light) shading. Anomalies are calculated as departures from the 1981-2010 base period monthly means.
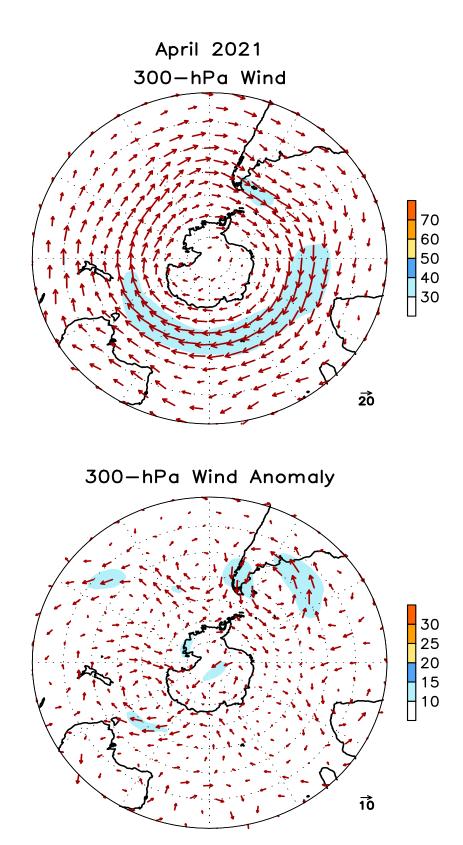
FIGURE E15. Southern Hemisphere mean and anomalous 500-hPa geopotential height (CDAS/Reanalysis) for APR 2021. Mean heights are denoted by solid contours drawn at an interval of 6 dam. Anomaly contour interval is 3 dam with values less (greater) than -3 dam (3 dam) indicated by dark (light) shading. Anomalies are calculated as departures from the 1981-2010 base period monthly means.

April 2021
300-hPa Wind

300-hPa Wind Anomaly

FIGURE E16. Southern Hemisphere mean (left) and anomalous (right) 300-hPa vector wind (CDAS/Reanalysis) for APR 2021. Mean (anomaly) isotach contour interval is 10 (5) ms^{-1}. Values greater than 30 ms^{-1} (left) and 10 ms^{-1} (rights) are shaded. Anomalies are departures from the 1981-2010 base period monthly means.

April 2021
500−hPa: Percentage of Anomaly Days

FIGURE E17. Southern Hemisphere percentage of days during APR 2021 in which 500-hPa height anomalies greater than 15 m (red) and less than -15 m (blue) were observed. Values greater than 70% are shaded and contour in-

April 2021
500-hPa Height Anomalies: 40°S

FIGURE E18. Southern Hemisphere: Daily 500-hPa height anomalies for APR 2021 averaged over the 5° latitude band centered on 40°S. Positive values are indicated by solid contours and dark shading. Negative values are indicated by dashed coutours and light shading. Contour interval is 60 m. Anomalies are departures from the 1981-2010 base period daily means.

April 2021
Height Anomalies

30-hPa

50-hPa

100-hPa

300-hPa

FIGURE S1. Stratospheric height anomalies (m) at selected levels for APR 2021. Positive values are indicated by solid contours and dark shading. Negative values are indicated by dashed contours and light shading. Contour interval is 60 m. Anomalies are calculated from the 1981-2010 base period means. Winter Hemisphere is shown.

FIGURE S2. Height-longitude sections during APR 2021 for height anomalies (contour) and temperature anomalies (shaded). In both panels, positive values are indicated by solid contours and dark shading, while negative anomalies are indicated by dashed contours and light shading. Contour interval for height anomalies is 60 m and for temperature anomalies is 2°C. Anomalies are calculated from the 1981-2010 base period monthly means. Winter Hemisphere is shown.

50hPa FMA Mean Temperature Anomalies

FIGURE S3. Seasonal mean temperature anomalies at 50-hPa for the latitude bands 65°–90°N, 25°–65°N, 25°N–25°S, 25°–65°S, 65°–90°S. The seasonal mean is comprised of the most recent three months. Zonal anomalies are taken from the mean of the entire data set.
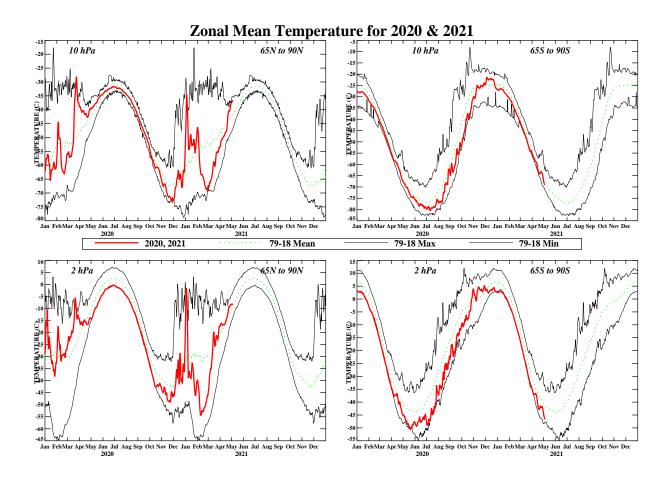
FIGURE S4. Daily mean temperatures at 10-hPa and 2-hPa (thick line) in the region 65°–90°N and 65°–90°S for the past two years. Dashed line depicts the 1981-2010 base period daily mean. Thin solid lines depict the daily extreme maximum and minimum temperatures.
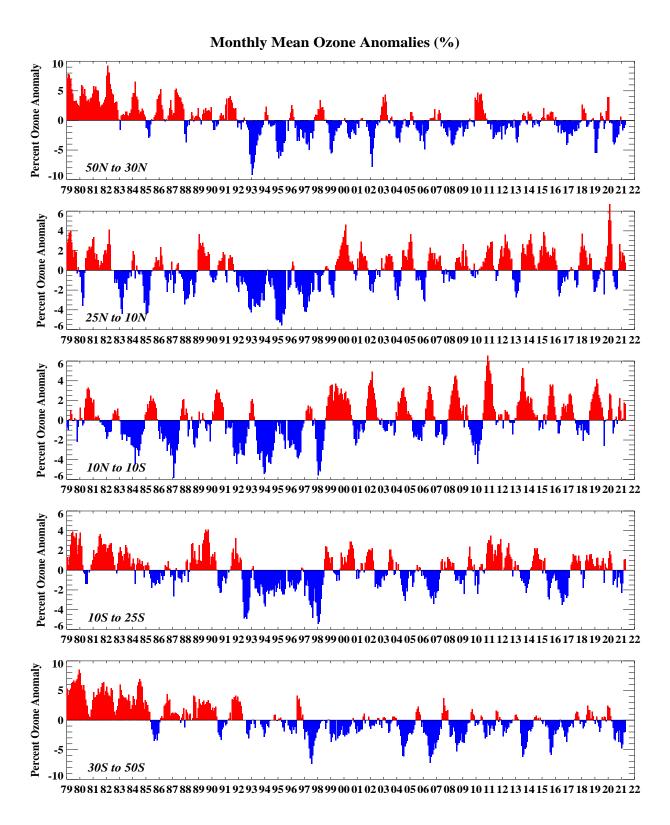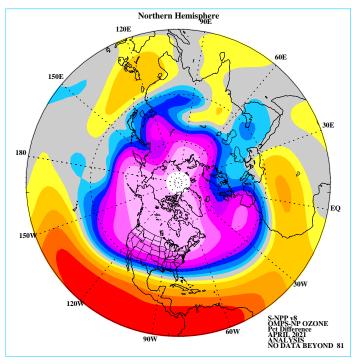
Monthly Mean Ozone Anomalies (%)

FIGURE S5. Monthly ozone anomalies (percent) from the long term monthly means for five zones: 50N-30N (NH mid-latitudes), 25N-10N (NH tropical surf zone), 10N-10S (Equatorial-QBO zone), 10S-25S (SH tropical surf zone), and 30S-50S (SH mid-latitudes). The long term monthly means are determined from the entire data set
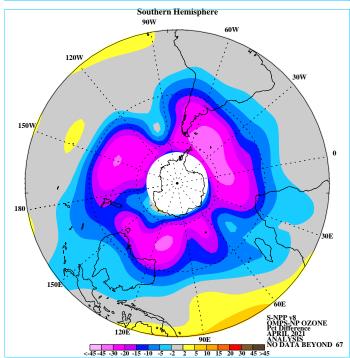
APRIL PERCENT DIFF (2021 - AVG[79-86])

FIGURE S6. Northern (top) and Southern (bottom) Hemisphere total ozone anomaly (percent difference from monthly mean for the period 1979-1986). The region near the winter pole has no SBUV/2 data.
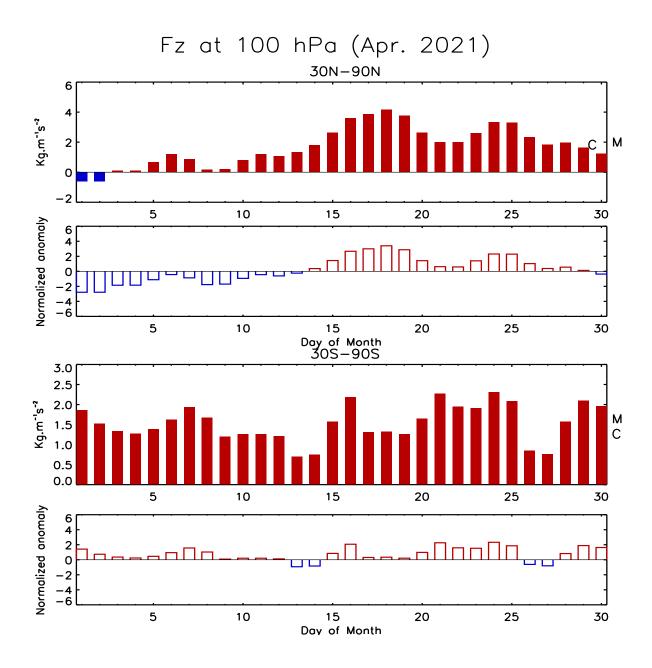
FIGURE S7. Daily vertical component of EP flux (which is proportional to the poleward transport of heat or upward transport of potential energy by planetary wave) at 100 hPa averaged over (top) 30°N–90°N and (bottom) 30°S–90°S for APR 2021. The EP flux unit (kg m^{-1} s^{-2}) has been scaled by multiplying a factor of the Brunt Vaisala frequency divided by the Coriolis parameter and the radius of the earth. The letter 'M' indicates the current monthly mean value and the letter 'C' indicates the climatological mean value. Additionally, the normalized departures from the monthly climatological EP flux values are shown.
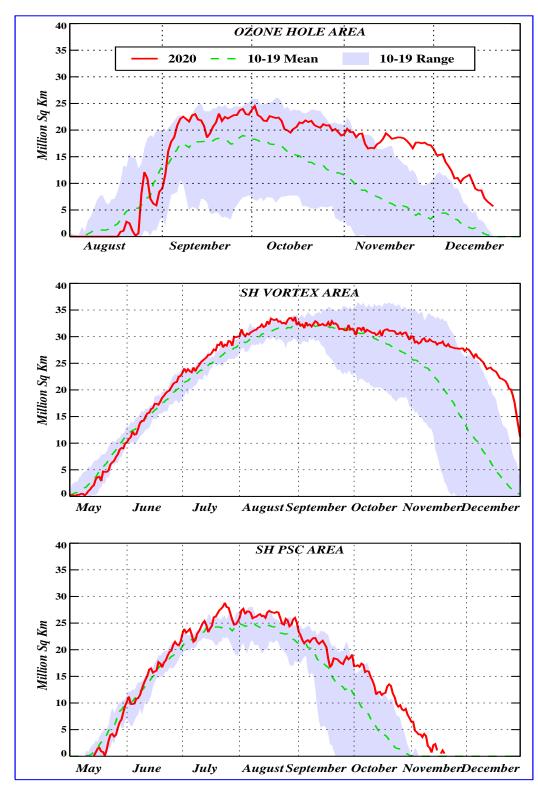
FIGURE S8. Daily time series showing the size of the SH polar vortex (representing the area enclosed by the 32 PVU contour on the 450K isentropic surface), and the areal coverage of temperatures < -78C on the 450K isentropic surface.
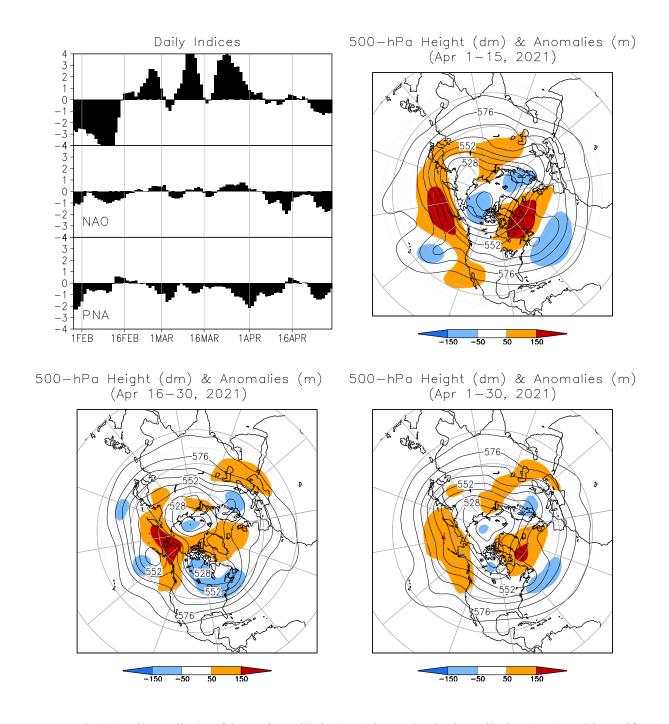
FIGURE A2.1. (a) Daily amplitudes of the Arctic Oscillation (AO) the North Atlantic Oscillation (NAO), and the Pacific-North American (PNA) pattern. The pattern amplitudes for the AO, (NAO, PNA) are calculated by projecting the daily 1000-hPa (500-hPa) height anomaly field onto the leading EOF obtained from standardized time- series of daily 1000-hPa (500-hPa) height for all months of the year. The base period is 1981–2010.

(b-d) Northern Hemisphere mean and anomalous 500-hPa geopotential height (CDAS/Reanalysis) for selected periods during APR 2021 are shown in the remaining 3 panels. Mean heights are denoted by solid contours drawn at an interval of 8 dam. Dark (light) shading corresponds to anomalies greater than 50 m (less than -50 m). Anomalies are calculated as departures from the 1981-2010 base period daily means.
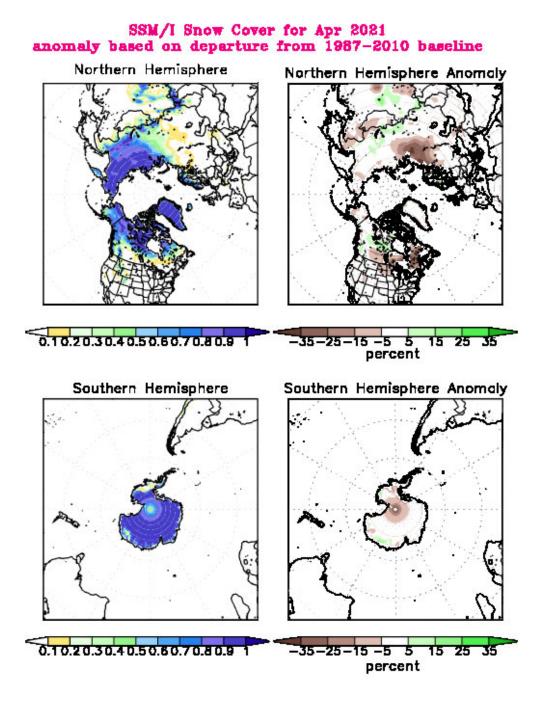
FIGURE A2.2. SSM/I derived snow cover frequency (%) (left) and snow cover anomaly (%) (right) for the month of APR 2021 based on 1987 - 2010 base period for the Northern Hemisphere (top) and Southern Hemisphere (bottom). It is generated using the algorithm described by Ferraro et. al, 1996, Bull. Amer. Meteor. Soc., vol 77, 891-905.